

# Dorrigo Marine Seismic Survey

---

## Oil Spill Modelling

**Prepared by:** RPS AUSTRALIA WEST PTY LTD  
Suite E1, Level 4  
140 Bundall Road  
Bundall, QLD 4217  
Australia

**T:** [REDACTED]  
**E:** [REDACTED]

**Author:** [REDACTED]

**Reviewed:** [REDACTED]

**Approved:** [REDACTED]

**No.:** MAQ0658J

**Version:** 0

**Date:** 6/04/18

**Prepared for:** 3D OIL LIMITED  
Level 5, 164 Flinders Lane  
Melbourne VIC 3000

**T:** [REDACTED]  
**E:** [REDACTED]  
**W:** www.3doil.com.au

RPS

## Document Status

| Version | Purpose of Document    | Approved by | Reviewed by | Review Date |
|---------|------------------------|-------------|-------------|-------------|
| 0       | Draft issued to client | [REDACTED]  | [REDACTED]  | 6/04/2018   |
|         |                        |             |             |             |
|         |                        |             |             |             |
|         |                        |             |             |             |

## Approval for issue

| Name       | Signature  | Date      |
|------------|------------|-----------|
| [REDACTED] | [REDACTED] | 6/04/2018 |

This report was prepared by [RPS Australia West Pty Ltd ('RPS')] within the terms of its engagement and in direct response to a scope of services. This report is strictly limited to the purpose and the facts and matters stated in it and does not apply directly or indirectly and must not be used for any other application, purpose, use or matter. In preparing the report, RPS may have relied upon information provided to it at the time by other parties. RPS accepts no responsibility as to the accuracy or completeness of information provided by those parties at the time of preparing the report. The report does not take into account any changes in information that may have occurred since the publication of the report. If the information relied upon is subsequently determined to be false, inaccurate or incomplete then it is possible that the observations and conclusions expressed in the report may have changed. RPS does not warrant the contents of this report and shall not assume any responsibility or liability for loss whatsoever to any third party caused by, related to or arising out of any use or reliance on the report howsoever. No part of this report, its attachments or appendices may be reproduced by any process without the written consent of RPS. All enquiries should be directed to RPS.

# Contents

|   |           |
|---|-----------|
| <b>EXECUTIVE SUMMARY</b> .....  | <b>7</b>  |
| <b>Background</b> .....   | <b>7</b>  |
| <b>Methodology</b> .....  | <b>7</b>  |
| <b>Oil Properties</b> .....   | <b>7</b>  |
| <b>Key Findings</b> .....   | <b>8</b>  |
| <b>1 INTRODUCTION</b> .....   | <b>9</b>  |
| <b>2 SCOPE OF WORK</b> .....  | <b>11</b> |
| <b>3 REGIONAL CURRENTS</b> .....  | <b>11</b> |
| <b>3.1 Tidal Currents</b> .....   | <b>12</b> |
| 3.1.1 Grid Setup .....  | 12        |
| 3.1.2 Tidal Conditions .....  | 14        |
| 3.1.3 Surface Elevation Validation .....  | 14        |
| <b>3.2 Ocean Currents</b> .....   | <b>18</b> |
| <b>3.3 Currents at the Release Site</b> .....   | <b>19</b> |
| <b>4 WINDS</b> .....  | <b>22</b> |
| <b>5 WATER TEMPERATURE AND SALINITY</b> .....   | <b>26</b> |
| <b>6 OIL SPILL MODEL - SIMAP</b> .....  | <b>27</b> |
| <b>6.1 Stochastic Modelling</b> .....   | <b>27</b> |
| <b>6.2 Sea surface, Shoreline and In-Water Thresholds</b> .....   | <b>28</b> |
| 6.2.1 Sea surface Exposure Thresholds .....   | 28        |
| 6.2.2 Shoreline Contact Threshold .....   | 29        |
| 6.2.3 Water Column Exposure Thresholds .....  | 30        |
| <b>6.3 Exposure Calculation</b> .....   | <b>32</b> |
| <b>6.4 Receptors Assessed</b> .....   | <b>33</b> |
| <b>7 OIL PROPERTIES</b> .....   | <b>35</b> |
| <b>8 MODEL SETTINGS</b> .....   | <b>37</b> |
| <b>9 INTERPRETING MODELLING RESULTS</b> .....   | <b>38</b> |
| <b>10 RESULTS: 400M<sup>3</sup> SURFACE RELEASE OF MDO FROM A VESSEL COLLISION WITHIN THE DORIGO MARINE SEISMIC SURVEY AREA</b> ..... | <b>40</b> |
| <b>10.1 Sea Surface Exposure and Shoreline Contact</b> .....  | <b>40</b> |
| <b>10.2 Subsurface Exposure</b> .....   | <b>52</b> |
| 10.2.1 Dissolved Aromatics .....  | 52        |
| 10.2.2 Entrained Hydrocarbons .....   | 52        |
| <b>11 REFERENCES</b> .....  | <b>55</b> |

## Tables

|          |   |    |
|----------|---|----|
| Table 1  | Dorrigo Operational Area Coordinates.....   | 9  |
| Table 2  | Statistical comparison between the observed and predicted surface elevations. ....  | 15 |
| Table 3  | Predicted monthly average and maximum surface current speeds near the release site. The data was derived by combining the HYCOM ocean data and HYDROMAP tidal data from 2008-2012 (inclusive). .... | 19 |
| Table 4  | Predicted monthly average and maximum winds for the wind node within the operational area. Data derived from CFSR hindcast model from 2008-2012 (inclusive).....                                    | 23 |
| Table 5  | Monthly average sea surface temperature and salinity at the release site.....   | 26 |
| Table 6  | The Bonn Agreement Oil Appearance Code .....  | 28 |
| Table 7  | Thresholds used to classify the zones of sea surface exposure .....   | 29 |
| Table 8  | Thresholds use to assess shoreline contact.....   | 30 |
| Table 9  | Dissolved aromatic threshold values applied as part of the modelling study .....  | 31 |
| Table 10 | Entrained hydrocarbon threshold values applied as part of the modelling study. Thresholds based on OSPAR guidelines.....  | 31 |
| Table 11 | Physical characteristics.....   | 35 |
| Table 12 | Boiling point ranges.....   | 35 |
| Table 13 | Summary of the oil spill model settings used in this assessment. ....   | 37 |
| Table 14 | Summary of potential zones of sea surface exposure at each surface oil threshold.....   | 41 |
| Table 15 | Summary of shoreline contact across all shorelines.....   | 41 |
| Table 16 | Summary of the potential sea surface exposure to receptors from October to April. ....  | 42 |
| Table 17 | Summary of shoreline contact to individual shoreline receptors.....   | 43 |
| Table 18 | Maximum exposure to entrained hydrocarbons and sea surface probability. ....  | 53 |

## Figures

|           |  |    |
|-----------|--|----|
| Figure 1  | Location of the release points used in the study.....  | 10 |
| Figure 2  | Map showing a zoomed in view of the hydrodynamic model domain. Higher resolution areas are shown by the denser mesh zones. ....  | 13 |
| Figure 3  | Map showing the bathymetry used in the hydrodynamic model. ....  | 13 |
| Figure 4  | Comparison between predicted (blue line) and observed (red line) surface elevation variation at Eden (top) and Burnie (bottom), between the 1 <sup>st</sup> of February and the 1 <sup>st</sup> March 2013. ....   | 16 |
| Figure 5  | Comparison between predicted (red line) and observed (blue line) surface elevation variation at Pirates Bay between the 1 <sup>st</sup> of February and the 1 <sup>st</sup> March 2013.....  | 17 |
| Figure 6: | Screenshot of the zoomed-in view (upper image) and large scale view (lower image) of predicted tidal current vectors. Note the density of the tidal vectors vary with the grid resolution, particularly along the coastline and around the islands. Colourations of individual vectors indicate current speed.....   | 17 |
| Figure 7  | Modelled surface ocean currents on the 12 <sup>th</sup> November 2013. Derived from the HYCOM ocean hindcast model. The colours of the vectors indicate current speed in m/s. ....   | 18 |
| Figure 8  | Monthly surface current rose plots near the release site (derived by combining the HYDROMAP tidal currents and HYCOM ocean currents for 2008 – 2012 inclusive). The colour key shows the current magnitude (m/s), the compass direction provides the current direction flowing TOWARDS and the length of the wedge gives the percentage of the record for a speed and direction combination. ....  | 20 |
| Figure 9  | Seasonal surface current rose plots near the release site (derived by combining the HYDROMAP tidal currents and HYCOM ocean currents for 2008 – 2012 inclusive). The colour key shows the current magnitude (m/s), the compass direction provides the current direction flowing TOWARDS and the length of the wedge gives the percentage of the record for a speed and direction combination. .... | 21 |
| Figure 10 | Sample of the CFSR modelled wind data used for the oil spill model. ....   | 22 |
| Figure 11 | Modelled monthly wind rose distributions from 2008–2012 (inclusive), for the wind node within the operational area. The colour key shows the wind magnitude, the compass direction provides the direction FROM and the length of the wedge gives the percentage of the record for a particular speed and direction combination. ....   | 24 |
| Figure 12 | Modelled seasonal wind rose distributions from 2008–2012 (inclusive), for the wind node within the operational area. Data is derived from CFSR model. The colour key shows the wind speed (knots), the compass direction provides the direction FROM and the length of the wedge gives the percentage of the record for a particular speed and direction combination.....                          | 25 |
| Figure 13 | Photographs showing the difference between oil colour and thickness on the sea surface (source: adapted from OilSpillSolutions.org 2015) .....   | 29 |
| Figure 14 | Example time series plot of concentration of entrained hydrocarbons (top) at a receptor, and exposure (bottom) with no deperuration (blue) and with deperuration (green).....  | 33 |
| Figure 15 | Marine parks and RAMSAR sites assessed for oil exposure. ....  | 34 |
| Figure 16 | Reefs, shoals and banks assessed for oil exposure.....   | 34 |
| Figure 17 | Weathering and fates graph, as a function of volume, under 5, 10 and 15 knot static wind conditions. Results are based on a 400 m <sup>3</sup> of MDO over 6 hours (tracked for 20 days).....  | 36 |
| Figure 18 | Zones of potential exposure on the sea surface.....  | 44 |
| Figure 19 | Probability of oil exposure on the sea surface above low exposure ( $\geq 1$ g/m <sup>2</sup> ). ....  | 45 |
| Figure 20 | Probability of oil exposure on the sea surface above moderate exposure ( $\geq 10$ g/m <sup>2</sup> ). ....  | 46 |
| Figure 21 | Probability of oil exposure on the sea surface above high exposure ( $\geq 25$ g/m <sup>2</sup> ). ....  | 47 |
| Figure 22 | Minimum time before oil exposure on the sea surface above low exposure ( $\geq 0.5$ g/m <sup>2</sup> ). ....   | 48 |
| Figure 23 | Minimum time before oil exposure on the sea surface above moderate exposure ( $\geq 10$ g/m <sup>2</sup> ). ..   | 49 |

|           |   |    |
|-----------|---|----|
| Figure 24 | Minimum time before oil exposure on the sea surface above high exposure ( $\geq 25$ g/m <sup>2</sup> )..... | 50 |
| Figure 25 | Maximum potential shoreline loading from October to April. ....   | 51 |
| Figure 26 | Biologically important areas for the antipodean albatross assessed for oil exposure. ....                   | 60 |
| Figure 27 | Biologically important areas for the australasian gannet assessed for oil exposure .....                    | 60 |
| Figure 28 | Biologically important areas for the black-faced cormorant assessed for oil exposure .....                  | 61 |
| Figure 29 | Biologically important areas for the bullers albatross assessed for oil exposure. ....                      | 61 |
| Figure 30 | Biologically important areas for the campbell albatross assessed for oil exposure.....                      | 62 |
| Figure 31 | Biologically important areas for the common diving petrel assessed for oil exposure .....                   | 62 |
| Figure 32 | Biologically important areas for the indian yellow-nosed albatross assessed for oil exposure ...            | 63 |
| Figure 33 | Biologically important areas for the little penguin assessed for oil exposure .....                         | 63 |
| Figure 34 | Biologically important areas for the pygmy blue whale assessed for oil exposure .....                       | 64 |
| Figure 35 | Biologically important areas for the short-tailed shearwater assessed for oil exposure .....                | 64 |
| Figure 36 | Biologically important areas for the shy albatross assessed for oil exposure .....                          | 65 |
| Figure 37 | Biologically important areas for the southern right whale assessed for oil exposure .....                   | 65 |
| Figure 38 | Biologically important areas for the wandering albatross assessed for oil exposure .....                    | 66 |
| Figure 39 | Biologically important areas for the white shark assessed for oil exposure .....                            | 66 |
| Figure 40 | Biologically important areas for the white-faced storm-petrel assessed for oil exposure .....               | 67 |

# Executive Summary

---

## Background

3D Oil commissioned RPS to carry out quantitative oil spill modelling to assess the potential risk of a hydrocarbon release during marine seismic survey operations and, to assist in the development of the Environmental Plan (EP) and Oil Pollution Emergency Plan (OPEP). 3D Oil is proposing to conduct the Dorrigo three-dimensional (3D) marine seismic survey of Exploration Permit T/49P. Operations are predicted to commence between October 2018 and April 2019. The proposed area of operation is located approximately 18 km west of King Island and 56 km off Cape Otway in the Commonwealth waters.

Stochastic modelling was conducted to assess the risk and potential exposure to surrounding waters and contact to the shorelines throughout the proposed operational period following a hypothetical yet plausible scenario:

- A 400 m<sup>3</sup> surface release of marine diesel oil over 6 hours, to represent a vessel collision incident, from 100 randomly selected release sites within the permit area.

The SIMAP system, the methods and analysis presented herein use modelling algorithms which have been anonymously peer reviewed and published in international journals. Further, RPS APASA warrants that this work meets and exceeds the ASTM Standard F2067-13 "*Standard Practice for Development and Use of Oil Spill Models*".

Note that the modelling does not take into consideration any of the spill prevention, mitigation and response capabilities that might be in place during the operations. The modelling makes no allowance for intervention following a spill to reduce volumes and/or prevent hydrocarbons from reaching sensitive areas.

## Methodology

The modelling study was carried out in several stages. Firstly, a five-year current dataset (2008–2012) that includes the combined influence of ocean currents from the HYCOM model and tidal currents from the HYDROMAP model was developed. Secondly, high-resolution local winds from the CFSR model and detailed hydrocarbon characteristics were used as inputs in the three-dimensional oil spill model (SIMAP) to simulate the drift, spread, weathering and fate of the spilled oils.

As spills can occur during any set of wind and current conditions, modelling was conducted using a stochastic (random or non-deterministic) approach, which involved running 100 spill simulations per release site initiated at random start times, using the same release information (spill volume, duration and composition of the oil). This ensured that each simulation was subject to different wind and current conditions and, in turn, movement and weathering of the oil.

## Oil Properties

The oil type used for the vessel collision incident was a marine diesel oil (MDO). The MDO is a medium grade oil (Classified as a Group II oil) used in the maritime industry. It has a density of 829.1 kg/m<sup>3</sup> (API of 37.6), a pour point (-14°C) and a dynamic viscosity at 25°C (4.0 cP), which indicates that this oil will spread quickly when spilled at sea and thin out to low thickness levels; which increases the rate of evaporation. The marine diesel has a strong tendency to entrain into the upper water column in the presence of moderate winds and breaking waves (>12 knots) but re-floats to the surface when the conditions calm which delays the evaporation process. Approximately, 5% (by mass) of the oil is considered "persistent hydrocarbons". These

oil properties categorise MDO as a Group 2 oil according to the International Tanker Owners Pollution Federation (ITOPF, 2014).

## Key Findings

- The maximum distance from a release site for potential of low, moderate and high surface exposure were 48 km (South) 14km (South) and 17km (East), respectively.
- Modelling demonstrated a 2% probability of contact to any shoreline and an absolute minimum time for visible oil to come ashore of approximately 30 hours and had a maximum onshore volume of 30 m<sup>3</sup>.
- Surface oil exposure was predicted to influence many Biologically Important Areas, due to the operational area overlapping these regions.
- King Island was the only shoreline shown to be impacted, with a 2% probability and a peak volume of 30 m<sup>3</sup> onshore across a maximum length of 8 km.
- No marine diesel oil was shown to persist on the water surface beyond 5 days at visible levels;
- Low level of entrained hydrocarbons is shown to occasionally impact on bird foraging areas including 6 species of albatross, 2 species of shearwater and 2 species of petrel.
- No zones of exposure to entrained hydrocarbons were observed at or above the moderate exposure threshold of 67,200 ppb.hrs, under any of the environmental conditions or depth profiles assessed; and
- No zones of exposure to dissolved aromatics above the low exposure thresholds of 576 ppb.hrs were observed.

# 1 Introduction

3D Oil commissioned RPS to carry out quantitative oil spill modelling to assess the potential risk of a hydrocarbon release during marine seismic survey operations and to assist in the development of the Environmental Plan (EP) and Oil Pollution Emergency Plan (OPEP). 3D Oil is proposing to conduct the Dorrigo three-dimensional (3D) marine seismic survey of Exploration Permit T/49P. Operations are predicted to commence between October 2018 and April 2019. The proposed area of operation is located approximately 18 km west of King Island and 56 km off Cape Otway in the Commonwealth waters.

Stochastic modelling was conducted to assess the risk and potential exposure to surrounding waters and contact to the shorelines throughout the proposed operational period following a hypothetical yet plausible scenario:

- A 400 m<sup>3</sup> surface release of marine diesel oil over 6 hours, to represent a vessel collision incident, from 100 randomly selected release sites within the permit area.

The SIMAP system, the methods and analysis presented herein use modelling algorithms which have been anonymously peer reviewed and published in international journals. Further, RPS APASA warrants that this work meets and exceeds the ASTM Standard F2067-13 “*Standard Practice for Development and Use of Oil Spill Models*”.

The modelling study was carried out in several stages. Firstly, a five-year current dataset (2008–2012) that includes the combined influence of ocean currents from the HYCOM model and tidal currents from the HYDROMAP model was developed. Secondly, high-resolution local winds from the CFSR model and detailed hydrocarbon characteristics were used as inputs in the three-dimensional oil spill model (SIMAP) to simulate the drift, spread, weathering and fate of the spilled oils.

As spills can occur during any set of wind and current conditions, modelling was conducted using a stochastic (random or non-deterministic) approach, which involved running 100 spill simulations at 100 randomly selected spill locations within the area of proposed operation. The simulations were initiated at random start times, using the same release information (spill volume, duration and composition of the oil). This ensured that each simulation was subject to different wind and current conditions and, in turn, movement and weathering of the oil.

Note that the modelling does not take into consideration any of the spill prevention, mitigation and response capabilities that might be in place during the operations. The modelling makes no allowance for intervention following a spill to reduce volumes and/or prevent hydrocarbons from reaching sensitive areas.

**Table 1 Dorrigo Operational Area Coordinates**

| Corner | Latitude             | Longitude           |
|--------|----------------------|---------------------|
| 1      | -40° 24' 35.97968" S | 143°38' 19.69206" E |
| 2      | -40° 25' 5.07109" S  | 143°11' 36.73302"E  |
| 3      | -39° 23' 8.67191" S  | 143° 9' 56.16522" E |
| 4      | -39° 22' 40.52208" S | 143°36' 23.83582" E |

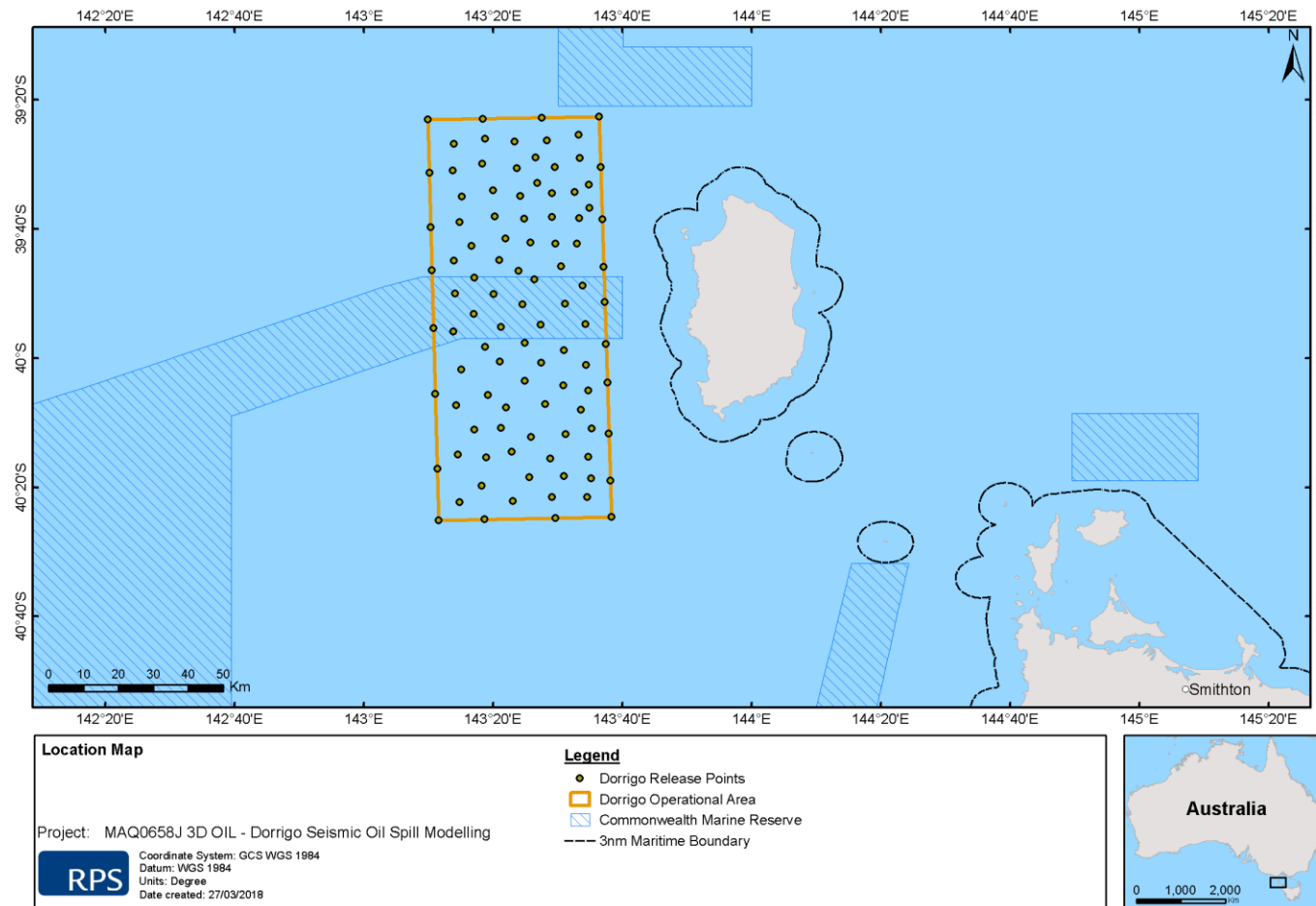


**Figure 1 Location of the release points used in the study**

## 2 Scope of Work

---

The scope of work included the following components:

1. Generate five years of net currents from 2008 to 2012 (inclusive) that include the combined influence of ocean and tidal currents.
2. Use high-resolution wind data, current data and hydrocarbon characteristics as input into the 3-dimensional oil spill model, SIMAP to model the movement, spreading, entrainment, weathering and potential shoreline contact by the hydrocarbon over time;
3. Use SIMAP's stochastic model (also known as a probability model) to calculate exposure to surround waters and shoreline. This involved running 100 spill simulations at 100 randomly selected spill locations within the area of proposed operation. The simulations were initiated at random start times, using the same release information (spill volume, duration and composition of the oil). This ensured that each simulation was subject to different wind and current conditions and, in turn, movement and weathering of the oil.

## 3 Regional Currents

---

Bass Strait is a sea strait separating Tasmania from the southern Australian mainland, specifically the state of Victoria. The strait is a relatively shallow area of the continental shelf, connecting the southeast Indian Ocean with the Tasman Sea. Bass Strait has a reputation for high winds and strong tidal currents (Jones, 1980). Currents within the strait are primarily driven by tides, winds and density driven flows. The Otway Basin is part of the Western field of the Bass Strait and lies along a north-west to south-east axis. It is approximately 500 km long and extends from Cape Jaffa in South Australia to north-west Tasmania and forms part of the Australian Southern Rift System.

The varied geography and bathymetry of the region, in addition to the forcing of the south-eastern Indian Ocean and local meteorology lead to complex shelf and slope circulation patterns (Middleton and Bye, 2007). Two important currents influencing the region, and contributing to the great complexity of its oceanography, include the Leeuwin and South Australian Currents:

- Leeuwin Current (LC) - This current originates from the tropical waters of the Indian Ocean and migrates along the continental shelf break east as far as 130° E. It passes from west to east in a narrow band predominantly (though not exclusively) during winter months (Rochford, 1986), when its velocity is at a maximum.
- South Australian Current (SAC) - During winter the SAC moves dense, salty, warmer water eastward from the Great Australian Bight into the western margin of the Bass Strait (Sandery and Kampf, 2007). In winter and spring, waters within the strait are well mixed with no obvious stratification, while during summer the central regions of the strait become stratified (Baines and Fandry 1983; Middleton and Black 1994).

To accurately describe the variability in currents between the inshore and offshore region, a hybrid regional data set was developed by combining deep ocean predictions obtained from HYCOM (Hybrid Coordinate Ocean Model) with surface tidal currents developed by RPS APASA. The following sections provide a summary of the hybrid regional data set.

### 3.1 Tidal Currents

The effects of tides were generated using RPS ASA's advanced ocean/coastal model, HYDROMAP. The HYDROMAP model has been thoroughly tested and verified through field measurements throughout the world over the past 26 years (Isaji and Spaulding, 1984; Isaji et al., 2001; Zigic et al., 2003). In fact, HYDROMAP tidal current data has been used as input to forecast (in the future) and hindcast (in the past) oil spills in Australian waters and forms part of the Australian National Oil Spill Emergency Response System operated by AMSA (Australian Maritime Safety Authority).

HYDROMAP employs a sophisticated sub-gridding strategy, which supports up to six levels of spatial resolution, halving the grid cell size as each level of resolution is employed. The sub-gridding allows for higher resolution of currents within areas of greater bathymetric and coastline complexity, and/or of particular interest to a study.

The numerical solution methodology follows that of Davies, 1977a, 1977b with further developments for model efficiency by Owen, 1980 and Gordon, 1982. A more detailed presentation of the model can be found in Isaji and Spaulding, 1984, Isaji et al., 2001.

#### 3.1.1 Grid Setup

HYDROMAP was used to set-up a domain that extended 1,150 km (east-west) by 1,095 km (north-south). The domain was subdivided horizontally into a grid with 3 levels of resolution. The resolution of the primary level was set at 8 km. The resolution of the first, second and third levels were 4 km, 2 km and 1 km, respectively. The finer grids were allocated in a step-wise fashion to more accurately resolve flows along the coastline, around islands and over more complex bathymetry. **Error! Reference source not found.** shows the tidal model grid domain, which extends over the Bass Strait from 140°E to 150°E longitude and 38°S to 42°S latitude.

To define the shape of the seafloor, the bathymetric data was obtained from extensive digitalised hydrographic charts, and was spatially interpolated to fill the entire model domain (refer **Error! Reference source not found.**). The minimum, average and maximum depths across the gridded region were 3 m, 503 m and 5,438 m, respectively.

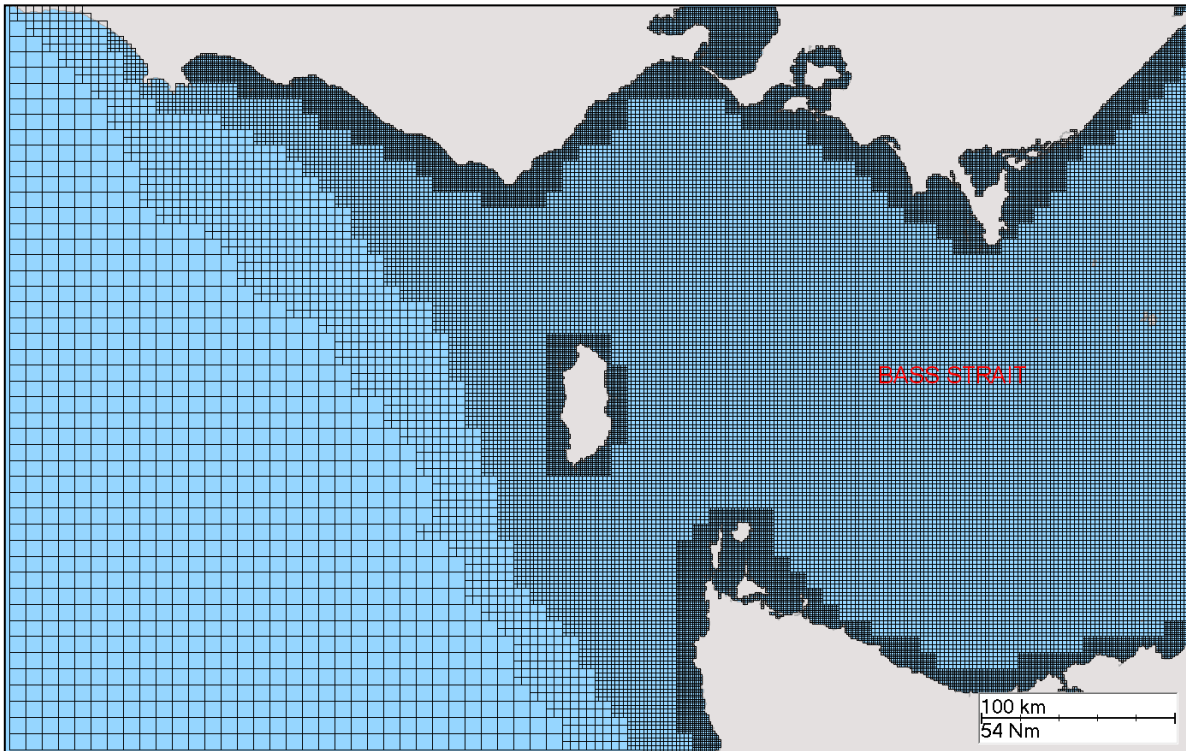


**Figure 2** Map showing a zoomed in view of the hydrodynamic model domain. Higher resolution areas are shown by the denser mesh zones.

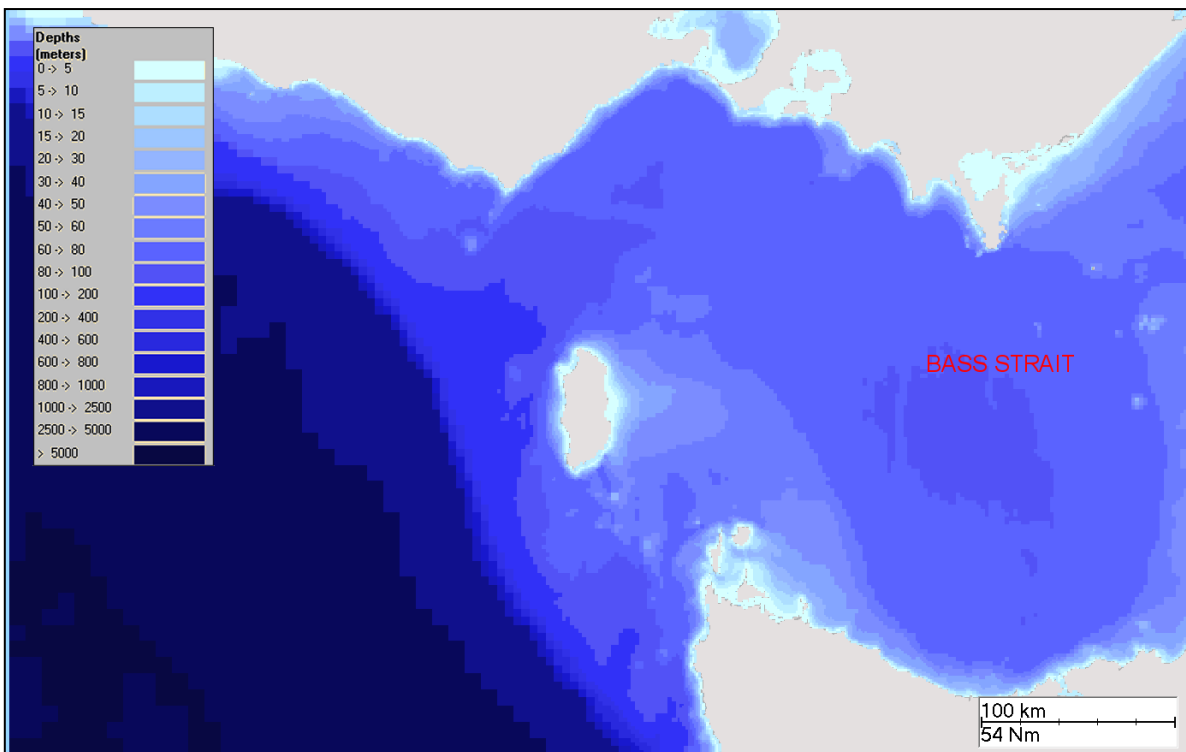


**Figure 3** Map showing the bathymetry used in the hydrodynamic model.

### 3.1.2 Tidal Conditions

The ocean boundary data for the regional model was obtained from satellite measured altimetry data (TOPEX/Poseidon 7.2) which provided estimates of the eight dominant tidal constituents at a horizontal scale of approximately 0.25 degrees. The eight major tidal constituents used were  $K_2$ ,  $S_2$ ,  $M_2$ ,  $N_2$ ,  $K_1$ ,  $P_1$ ,  $O_1$  and  $Q_1$ . Using the tidal data, surface heights were firstly calculated along the open boundaries, at each time step in the model.

The Topex-Poseidon satellite data has a resolution of 0.25 degrees (465 m) globally and is produced and quality controlled by NASA (National Aeronautics and Space Administration). The satellites, equipped with two highly accurate altimeters, capable of taking sea level measurements accurate to less than  $\pm 1$  cm, measured oceanic surface elevations (and the resultant tides) for over 13 years (1992–2005). In total these satellites carried out 62,000 orbits of the planet. The Topex-Poseidon tidal data has been widely used amongst the oceanographic community, being the subject of more than 2,100 research publications (e.g. Andersen, 1995; Ludicone et al., 1998; Matsumoto et al., 2000; Kostianoy et al., 2003; Yaremchuk and Tangdong, 2004; Qiu and Chen 2010). As such the Topex/Poseidon tidal data is considered suitably accurate for this study.

### 3.1.3 Surface Elevation Validation

To ensure that tidal predictions were accurate, predicted surface elevations were compared to data observed at eight locations.

Figure 4 and Figure 5 illustrate a comparison of the predicted and observed datasets for each location between the 1<sup>st</sup> February and 1<sup>st</sup> March 2013. As shown on the graphs, the model accurately reproduced the phase and amplitudes throughout the spring and neap tidal cycles.

To provide a statistical measure of the model's performance, the Index of Agreement (IOA - Willmott (1981)) and the Mean Absolute Error (MAE - Willmott (1982) and Willmott and Matsuura (2005)) were used.

The MAE is simply the average of the absolute values of the difference between the model-predicted (P) and observed (O) variables. It is a more natural measure of the average error (Willmott and Matsuura, 2005) and more readily understood

$$MAE = N^{-1} \sum_{i=1}^N |P_i - O_i|$$

The Index of Agreement (IOA) is determined by:

$$IOA = 1 - \frac{\sum |X_{model} - X_{obs}|^2}{\sum (|X_{model} - \bar{X}_{obs}| + |X_{obs} - \bar{X}_{obs}|)^2}$$

Where: X represents the variable being compared and the time mean of that variable. A perfect agreement exists between the model and field observations if the index gives an agreement value of 1 and complete disagreement will produce an index measure of 0 (Willmott, 1981). Willmott et al., (1985) also suggests that values meaningfully larger than 0.5 represent good model performance. Clearly, a greater IOA and lower MAE represent a better model performance.

Table 2 shows the IOA and MAE values for the selected locations. The average IOA across the 8 sites is 0.99 and the MAE values are relatively low considering the high tidal range at some sites; indicating the model is performing well.

**Table 2** Statistical comparison between the observed and predicted surface elevations.

| <b>Tide Station</b> | <b>IOA</b> | <b>MAE (m)</b> |
|---------------------|------------|----------------|
| Eden                | 0.99       | 1.04           |
| Burnie              | 0.96       | 1.15           |
| Pirates Bay         | 0.96       | 1.04           |

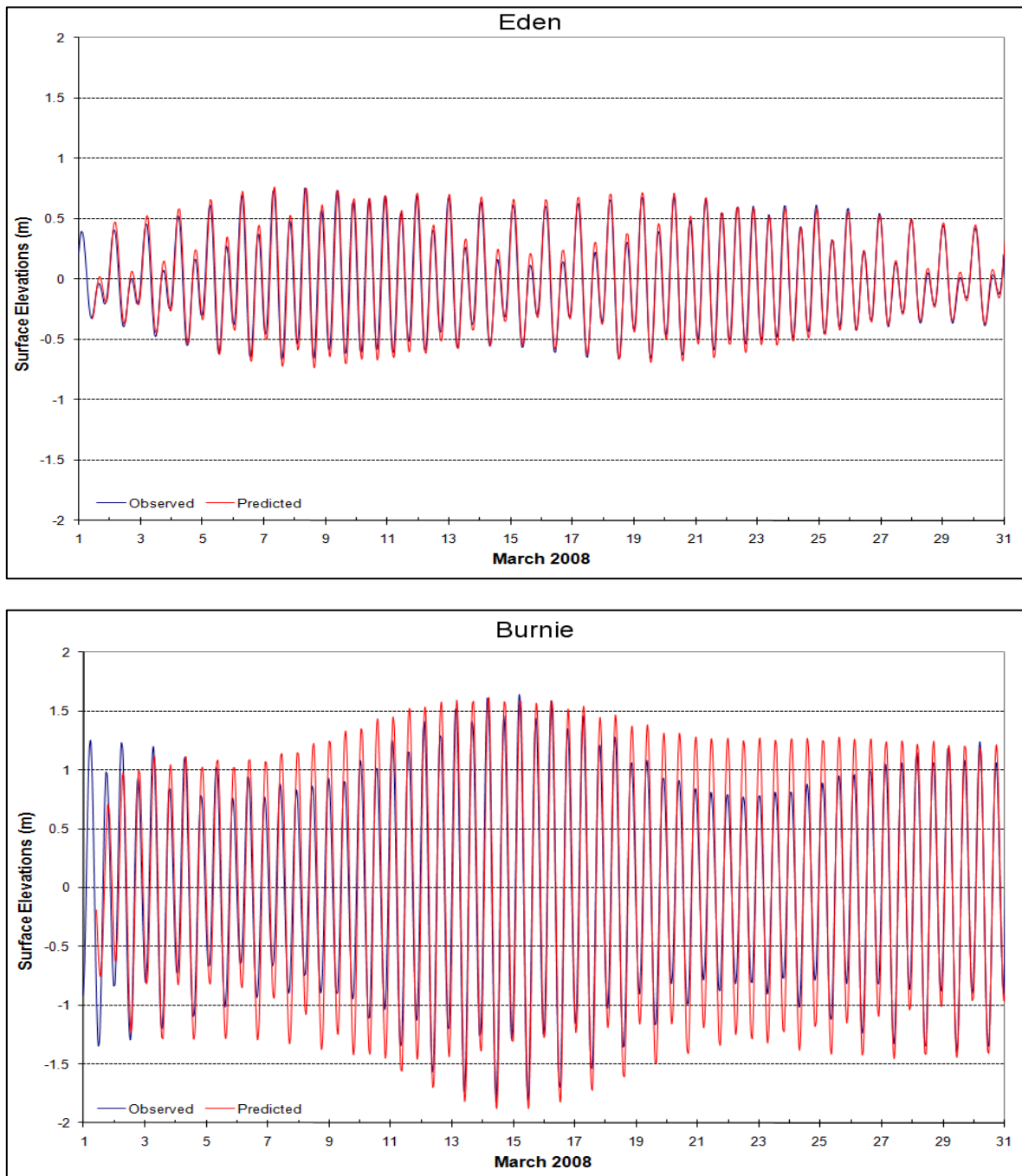


**Figure 4 Comparison between predicted (blue line) and observed (red line) surface elevation variation at Eden (top) and Burnie (bottom), between the 1<sup>st</sup> of February and the 1<sup>st</sup> March 2013.**

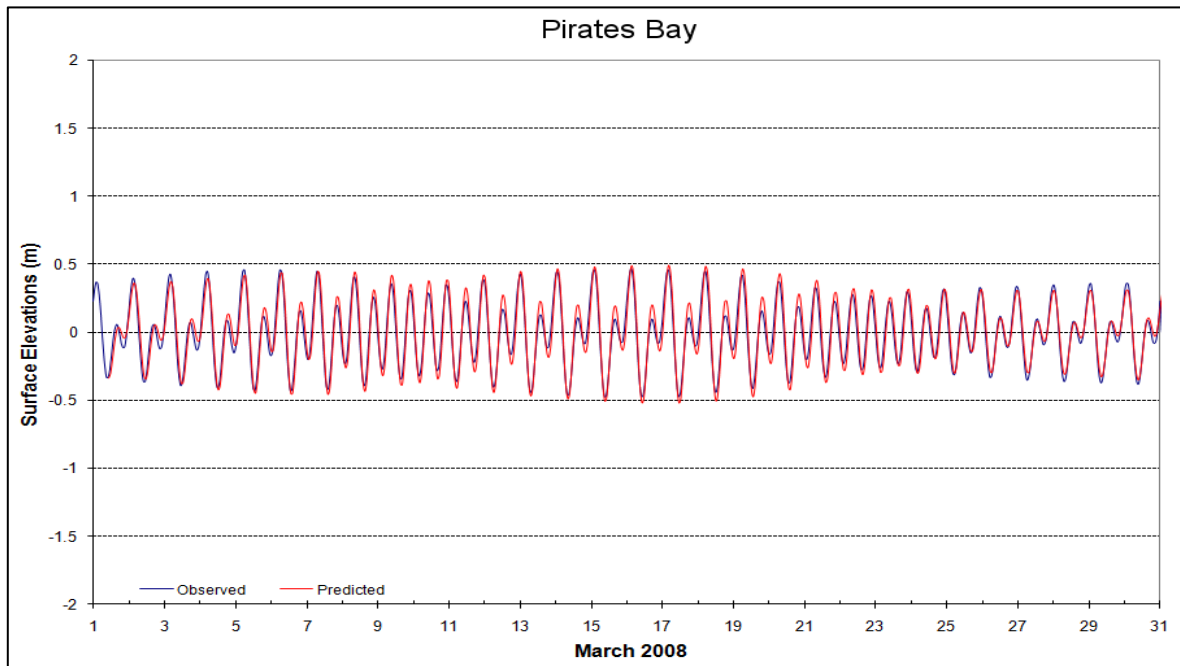


Figure 5 Comparison between predicted (red line) and observed (blue line) surface elevation variation at Pirates Bay between the 1<sup>st</sup> of February and the 1<sup>st</sup> March 2013.

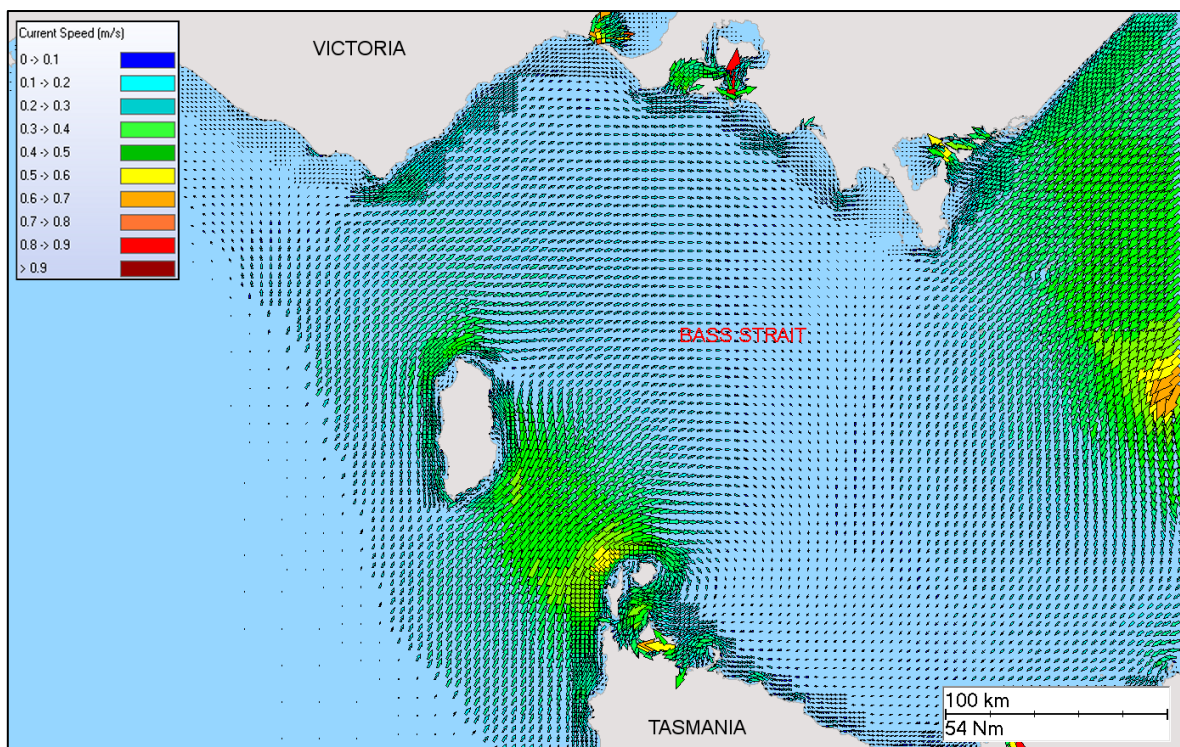


Figure 6: Screenshot of the zoomed-in view (upper image) and large scale view (lower image) of predicted tidal current vectors. Note the density of the tidal vectors vary with the grid resolution, particularly along the coastline and around the islands. Colourations of individual vectors indicate current speed.

### 3.2 Ocean Currents

Data describing the flow of ocean currents was obtained from HYCOM (Hybrid Coordinate Ocean Model) (see Chassignet et al. 2007), which is operated by the HYCOM Consortium, sponsored by the Global Ocean Data Assimilation Experiment (GODAE). HYCOM is a data-assimilative, three-dimensional ocean model that is run as a hindcast, assimilating time-varying observations of sea-surface height, sea-surface temperature and in-situ temperature and salinity measurements (Chassignet, et al., 2009). The HYCOM predictions for drift currents are produced at a horizontal spatial resolution of approximately 8.25 km (1/12<sup>th</sup> of a degree) over the region, at a frequency of once per day. HYCOM uses isopycnal layers in the open, stratified ocean, but uses the layered continuity equation to make a dynamically smooth transition to a terrain following coordinate in shallow coastal regions, and to z-level coordinates in the mixed layer and/or unstratified seas

For this study, the HYCOM hindcast currents were obtained for the years 2009 to 2013 (inclusive).

Figure 7 shows a screenshot of the predicted ocean currents at the surface during summer conditions (November). The colouration of the individual vectors indicates current speed (m/s).

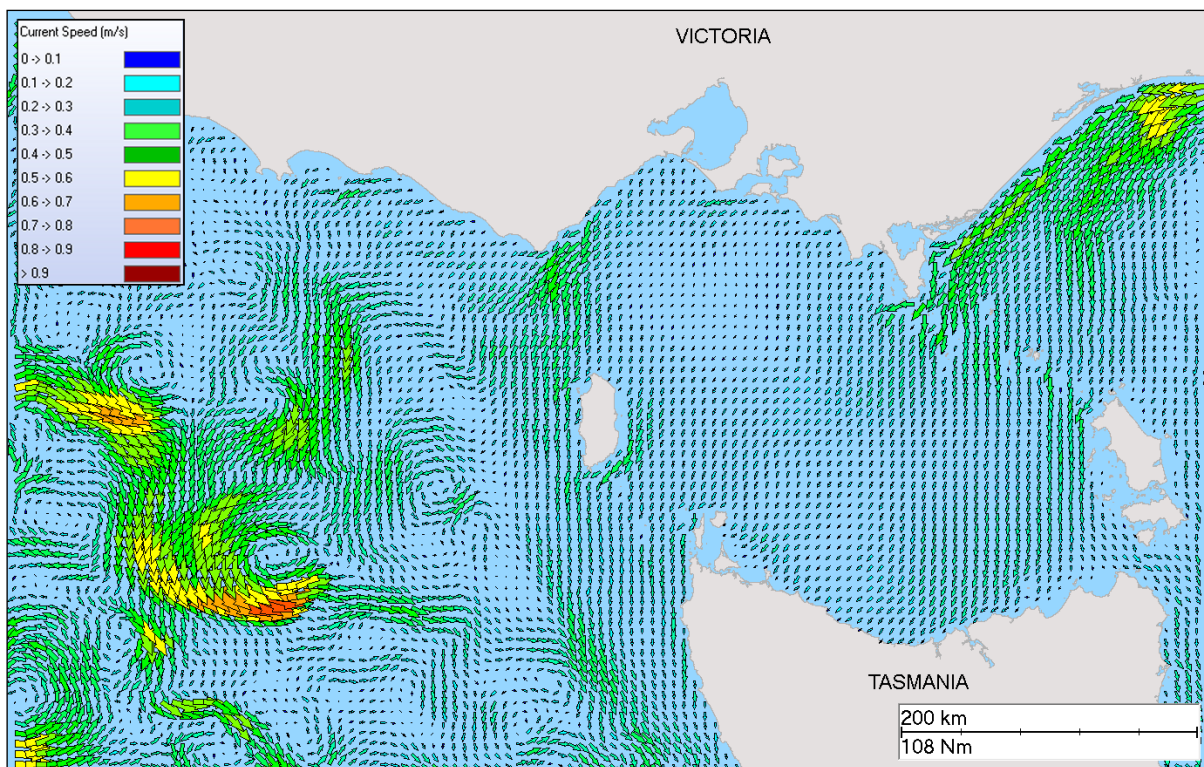


**Figure 7** Modelled surface ocean currents on the 12<sup>th</sup> November 2013. Derived from the HYCOM ocean hindcast model. The colours of the vectors indicate current speed in m/s.

### 3.3 Currents at the Release Site

Table 3 displays the average and maximum combined current speeds (ocean plus tides) adjacent the release sites. Figure 8 to Figure 9 show the monthly and seasonal surface current roses distributions resulting from the combination of HYCOM ocean current data and HYDROMAP tidal data in waters adjacent to the release sites.

Note the convention for defining current direction is the direction the current flows towards, which is used to reference current direction throughout this report. Each branch of the rose represents the currents flowing to that direction, with north to the top of the diagram. Sixteen directions are used. The branches are divided into segments of different colour, which represent the current speed ranges for each direction. Speed intervals of 0.2 m/s are used in these current roses. The length of each coloured segment is relative to the proportion of currents flowing within the corresponding speed and direction.

The data shows that the current speeds were consistent throughout the year ranging between 0.2 to 0.3 m/s and directions varied between months. The direction of current flow was predominantly east, a southeasterly influence was predicted for the months from March to November. A variable/northerly influence was predicted from December to February.

**Table 3 Predicted monthly average and maximum surface current speeds near the release site. The data was derived by combining the HYCOM ocean data and HYDROMAP tidal data from 2008-2012 (inclusive).**

|                | Average current speed (m/s) | Maximum current speed (m/s) | General Direction (Towards) |
|----------------|-----------------------------|-----------------------------|-----------------------------|
| January        | 0.2                         | 0.6                         | Variable                    |
| February       | 0.2                         | 0.8                         | Southwest- Northeast        |
| March          | 0.2                         | 0.7                         | East – Southeast            |
| April          | 0.2                         | 0.9                         | East – Southeast            |
| May            | 0.2                         | 0.6                         | East                        |
| June           | 0.2                         | 0.7                         | East                        |
| July           | 0.2                         | 0.8                         | East – Southeast            |
| August         | 0.3                         | 0.9                         | East – Southeast            |
| September      | 0.3                         | 0.7                         | East                        |
| October        | 0.2                         | 0.7                         | East                        |
| November       | 0.2                         | 0.6                         | East                        |
| December       | 0.2                         | 0.6                         | East - Northeast            |
| <b>Minimum</b> | <b>0.2</b>                  | <b>0.6</b>                  |                             |
| <b>Maximum</b> | <b>0.3</b>                  | <b>0.9</b>                  |                             |



**RPS Data Set Analysis**  
**Current Speed (m/s) and Direction Rose (All Records)**

Longitude = 143.40°E, Latitude = 39.89°S  
 Analysis Period: 01-Jan-2008 to 31-Dec-2012

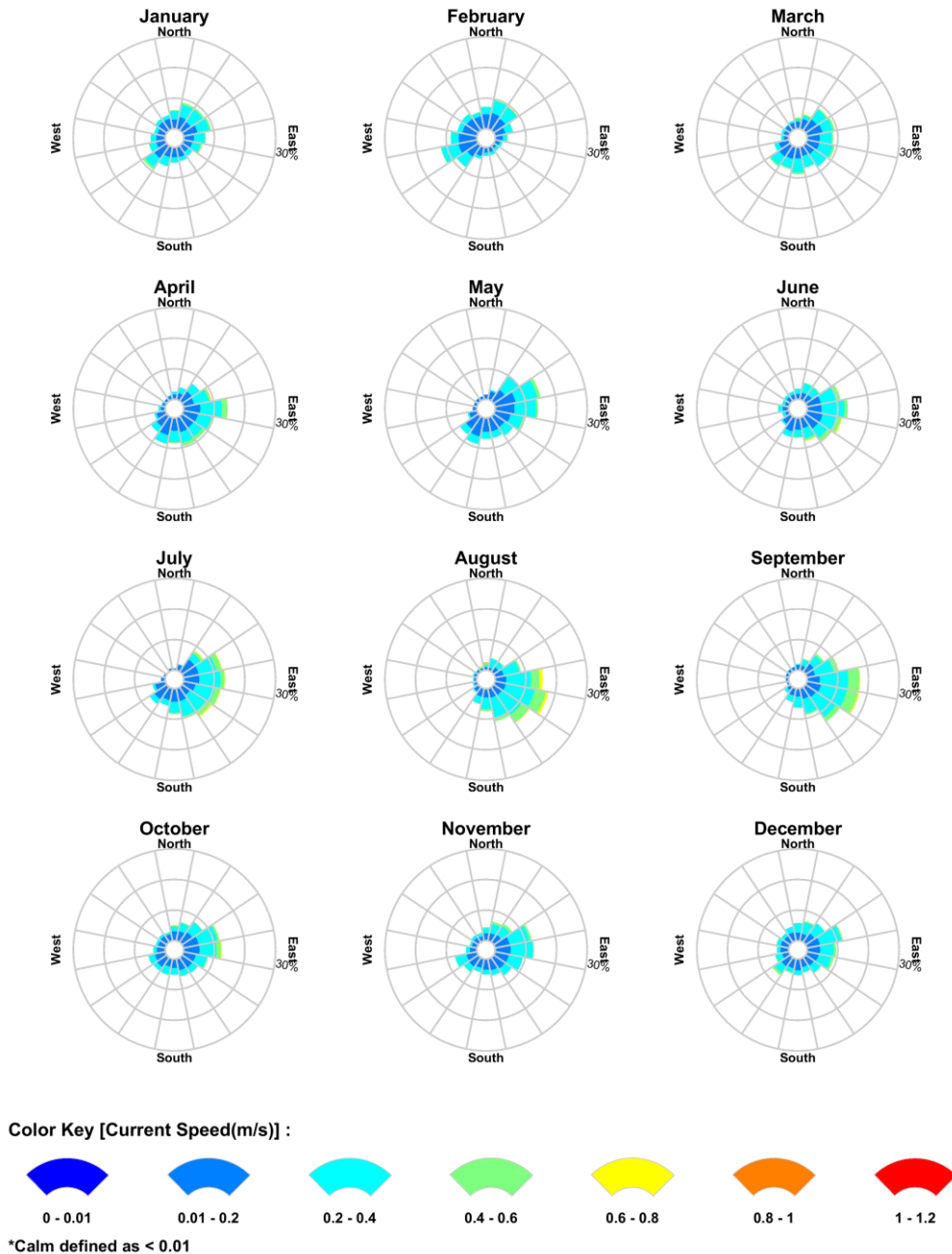


**Figure 8** Monthly surface current rose plots near the release site (derived by combining the HYDROMAP tidal currents and HYCOM ocean currents for 2008 – 2012 inclusive). The colour key shows the current magnitude (m/s), the compass direction provides the current direction flowing TOWARDS and the length of the wedge gives the percentage of the record for a speed and direction combination.



**RPS Data Set Analysis**

**Current Speed (m/s) and Direction Rose (All Records)**

Longitude = 143.40°E, Latitude = 39.89°S  
 Analysis Period: 01-Jan-2008 to 31-Dec-2012

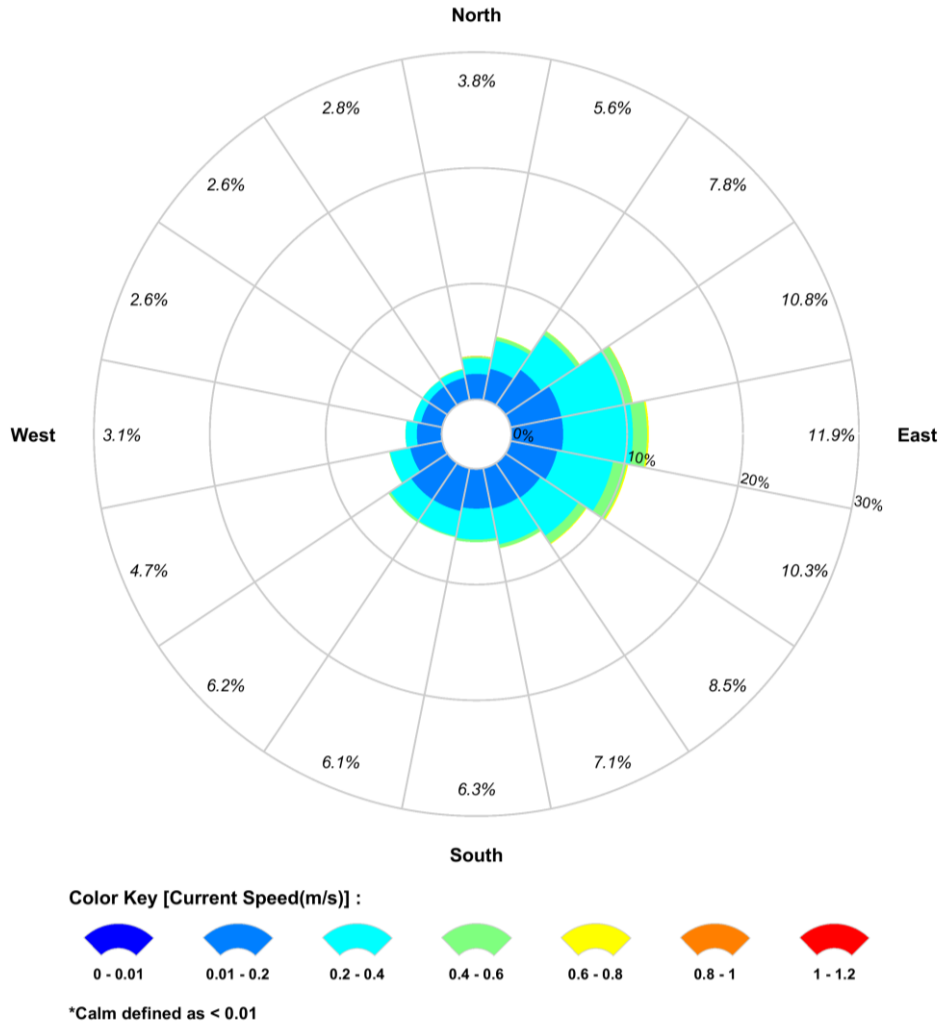


**Figure 9** Seasonal surface current rose plots near the release site (derived by combining the HYDROMAP tidal currents and HYCOM ocean currents for 2008 – 2012 inclusive). The colour key shows the current magnitude (m/s), the compass direction provides the current direction flowing TOWARDS and the length of the wedge gives the percentage of the record for a speed and direction combination.

## 4 Winds

High resolution wind data was sourced from the National Centre for Environmental Prediction (NCEP) Climate Forecast System Reanalysis (CFSR; see Saha et al., 2010). The CFSR wind model is a fully coupled, data-assimilative hind cast model representing the interaction between the earth's oceans, land and atmosphere. The gridded wind data output is available at  $\frac{1}{4}$  of a degree resolution ( $\sim 33$  km) and 1-hourly time intervals.

The CFSR wind data for the years 2008–2012 (inclusive) was compiled across the model domain. Figure 10 shows an example of the wind field used as input into the oil spill model.

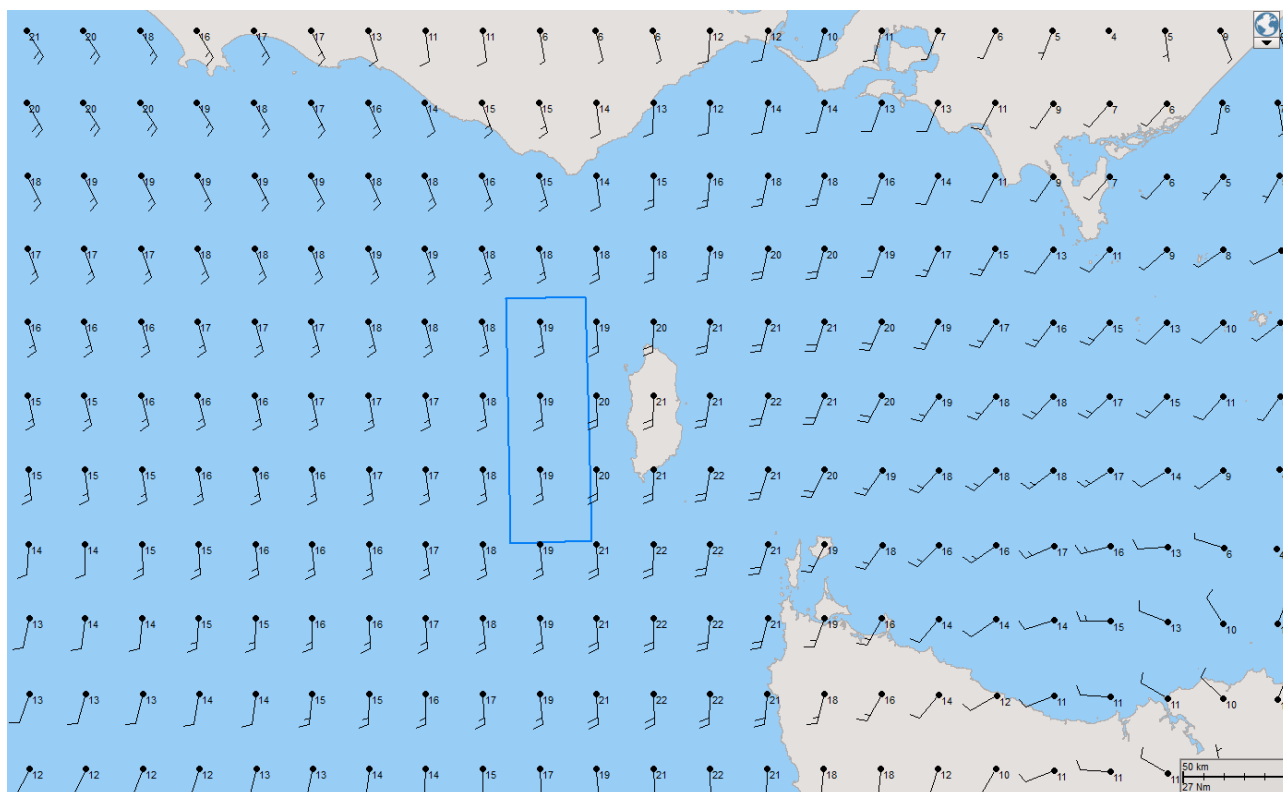


**Figure 10** Sample of the CFSR modelled wind data used for the oil spill model.

Figure 11 shows the monthly wind rose distribution, derived from the CFSR data for a node within the operational area.

Note that the atmospheric convention for defining wind direction, that is, the direction the wind blows from, is used to reference wind direction throughout this report. Each branch of the rose represents wind coming from that direction, with north to the top of the diagram. Sixteen directions are used. The branches are divided into segments of different colour, which represent wind speed ranges from that direction. Speed ranges of 2 knots are typically used in these wind roses. The length of each segment within a branch is proportional to the frequency of winds blowing within the corresponding range of speeds from that direction.

The wind node analysed demonstrated a predominant (general) wind direction from the west throughout most of the year, with January and February having slightly more dominant southerly direction.

The data indicated that winds across the region are relatively strong throughout the year with averages ranging from 14 – 20 knots and maximums reaching up to in the 50-knots, note however these maximum values are averaged over 3 hours and do not include any short-term wind gusts during severe storms.

**Table 4 Predicted monthly average and maximum winds for the wind node within the operational area. Data derived from CFSR hindcast model from 2008-2012 (inclusive).**

| Month          | Average wind (knots) | Maximum wind (knots) | General Direction (From) |
|----------------|----------------------|----------------------|--------------------------|
| January        | 14                   | 40                   | South – Southwest        |
| February       | 15                   | 42                   | South – Southeast        |
| March          | 15                   | 39                   | Southwest                |
| April          | 16                   | 50                   | Southwest                |
| May            | 16                   | 39                   | Southwest                |
| June           | 18                   | 43                   | Southwest - Northwest    |
| July           | 18                   | 45                   | Southwest - Northwest    |
| August         | 20                   | 45                   | West - Northwest         |
| September      | 19                   | 50                   | West                     |
| October        | 16                   | 37                   | Southwest                |
| November       | 15                   | 39                   | West                     |
| December       | 16                   | 39                   | West                     |
| <b>Minimum</b> | <b>14</b>            | <b>37</b>            |                          |
| <b>Maximum</b> | <b>20</b>            | <b>50</b>            |                          |



### RPS Data Set Analysis

#### Wind Speed (knots) and Direction Rose (All Records)

Longitude = 143.40°E, Latitude = 39.89°S  
 Analysis Period: 01-Jan-2008 to 31-Dec-2012

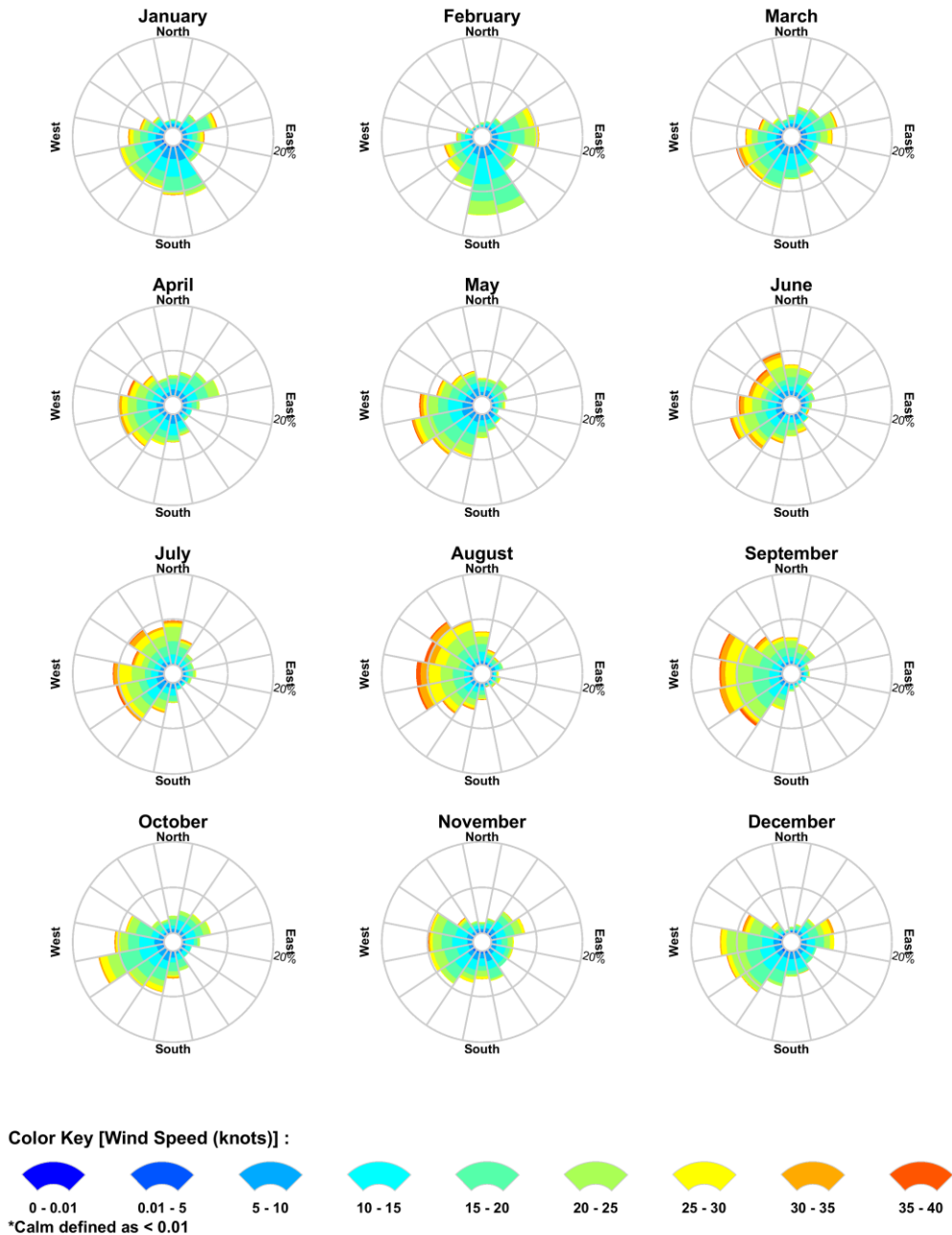


**Figure 11** Modelled monthly wind rose distributions from 2008–2012 (inclusive), for the wind node within the operational area. The colour key shows the wind magnitude, the compass direction provides the direction FROM and the length of the wedge gives the percentage of the record for a particular speed and direction combination.



**RPS Data Set Analysis**

**Wind Speed (knots) and Direction Rose (All Records)**

Longitude = 143.40°E, Latitude = 39.89°S  
 Analysis Period: 01-Jan-2008 to 31-Dec-2012

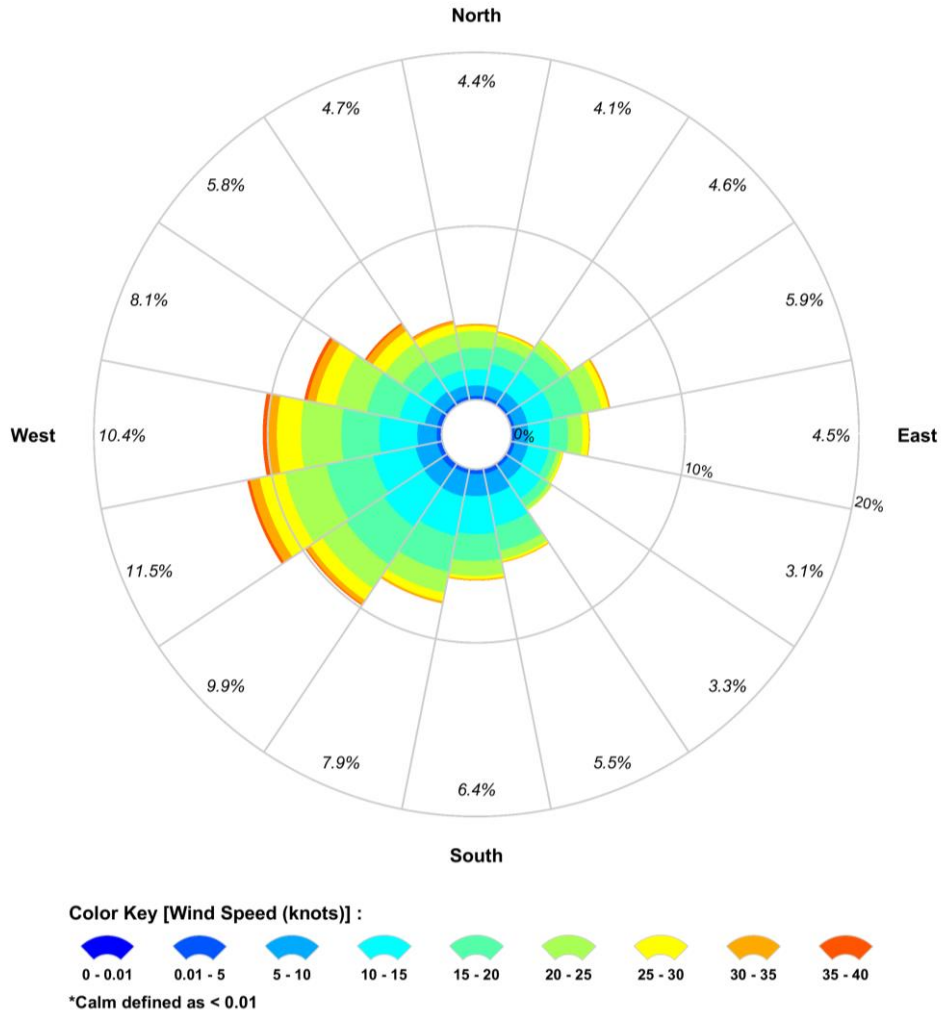


**Figure 12** Modelled seasonal wind rose distributions from 2008–2012 (inclusive), for the wind node within the operational area. Data is derived from CFSR model. The colour key shows the wind speed (knots), the compass direction provides the direction FROM and the length of the wedge gives the percentage of the record for a particular speed and direction combination.

## 5 Water Temperature and Salinity

Sea-surface water temperature and salinity, according to the National Oceanographic Data Centre – World Ocean Atlas ([www.metoc.gov.au](http://www.metoc.gov.au)), was found to be fairly consistent throughout the year, ranging between 13°C and 18°C, while salinity varied from 35.3 to 35.6 PSU.

These parameters were used as factors to inform the weathering, movement and evaporative loss of hydrocarbon spills in the surface and sub-surface thermo/halocline layers.

To account for depth-varying sea temperature and salinity, the modelling used monthly averaged sea temperature and salinity profiles at 10 m depth intervals throughout the water column. Table 5 presents the sea temperature and salinity of the surface layer (0-10 m).

**Table 5 Monthly average sea surface temperature and salinity at the release site.**

| Season    | Sea-Surface Temperature (°C) | Salinity (PSU) |
|-----------|------------------------------|----------------|
| January   | 16                           | 35.3           |
| February  | 18                           | 35.4           |
| March     | 17                           | 35.4           |
| April     | 17                           | 35.4           |
| May       | 15                           | 35.5           |
| June      | 15                           | 35.4           |
| July      | 14                           | 35.5           |
| August    | 14                           | 35.4           |
| September | 13                           | 35.4           |
| October   | 13                           | 35.4           |
| November  | 14                           | 35.6           |
| December  | 16                           | 35.4           |

## 6 Oil Spill Model - SIMAP

---

The oil spill modelling was performed using SIMAP. SIMAP is designed to simulate the fate and effects of spilled hydrocarbons for both the surface and subsurface releases (Spaulding et al., 1994; French et al., 1999; French-McCay, 2003; French-McCay, 2004; French-McCay et al., 2004; Spaulding, et al., 1994).

The SIMAP model calculates two components: (i) the transport, spreading, entrainment, evaporation and decay of surface oil slicks and, (ii) the entrained and dissolved hydrocarbons released from the slicks into the water column. Input specifications for oil-types include the density, viscosity, pour point, distillation curve (volume lost versus temperature) and the aromatic/aliphatic component ratios within given boiling point ranges.

The SIMAP trajectory model separately calculates the movement of the material that: (i) is on the water surface (as surface slicks), (ii) in the water column (as either entrained whole oil droplets or dissolved hydrocarbon), (iii) has stranded on shorelines, or (iv) that has precipitated out of the water column onto the seabed. The model calculates the transport of surface slicks from the combined forces exerted by surface currents and wind acting on the oil. Transport of entrained oil (oil that is below the water surface) is calculated using the currents only.

### 6.1 Stochastic Modelling

As spills can occur during any set of wind and current conditions, SIMAP's stochastic model was used to quantify the probability of exposure to the sea surface, in-water and shoreline contacts for a hypothetical spill scenario over a 5-year period.

For this assessment, a total of 100 single spill trajectories from 100 randomly selected spill locations within the intended operational area were run for the hypothetical scenario.

Each simulation had the same spill information (i.e. spill volume, duration and oil type) for each scenario but with varying start times, and in turn, the prevailing wind and current conditions. This approach ensures that the predicted transport and weathering of an oil slick is subject to a wide range of current and wind conditions.

During each spill trajectory, the model records the grid cells exposed to hydrocarbons, as well as the time elapsed. Once all the spill trajectories have been run, the model then combines the results from the individual simulations to determine the following:

- Maximum exposure (or load) observed on the sea surface;
- Minimum time before sea surface exposure;
- Probability of contact to any shorelines;
- Probability of contact to individual sections of shorelines;
- Maximum volume of oil that may contact shorelines from a single simulation;
- Maximum load that an individual shoreline may experience;
- Maximum exposure from entrained hydrocarbons observed in the water column; and
- Maximum exposure from dissolved aromatic hydrocarbons observed in the water column.

The stochastic model output does not represent the extent of any one spill trajectory (which would be significantly smaller) but rather provides a summary of all trajectories run for the scenario.

## 6.2 Sea surface, Shoreline and In-Water Thresholds

### 6.2.1 Sea surface Exposure Thresholds

The SIMAP model is able to track hydrocarbons to levels lower than biologically significant or visible to the naked eye. Therefore, reporting thresholds have been specified (based on the scientific literature) to account for “exposure” on the sea surface and “contact” to shorelines at meaningful levels.

To better assess the potential for sea surface exposure, each of the 100 spill trajectories was tracked to a minimum of 1 g/m<sup>2</sup>, which equates approximately to an average thickness of ~0.5 µm. Oil of this thickness is described as a silvery to rainbow sheen in appearance, according to the Bonn Agreement Oil Appearance Code (Bonn Agreement 2009) (refer to Table 6) and is also considered the practical limit of observing oil in the marine environment (AMSA, 2012). This threshold is considered below levels which would cause environmental harm and it is more indicative of the areas perceived to be affected due to its visibility on the sea surface and potential to trigger temporary closures of areas (i.e. fishing grounds) as a precautionary measure. Hence, the 0.5 g/m<sup>2</sup> threshold has been selected to define the zone of potential low exposure on the sea surface.

Ecological impact has been estimated to occur at 10 g/m<sup>2</sup> (~10 µm) according to French et al. (1996) and French-McCay (2009) (see references therein) as this level of oiling has been observed to mortally impact birds and other wildlife associated with the water surface. The 10 g/m<sup>2</sup> threshold has been selected to define the zone of potential moderate exposure on the sea surface.

Scholten et al. (1996) and Koops et al. (2004) indicated that a concentration of surface oil equal to 25 g/m<sup>2</sup> or greater would be harmful for all birds that contact the slick. Exposure to oil concentrations at or above this threshold is used to define the zone of potential high exposure.

Table 7 defines the thresholds used to classify the zones of sea surface exposure. Figure 13 shows photographs highlighting the difference in appearance between a silvery sheen, rainbow sheen and metallic sheen.

**Table 6 The Bonn Agreement Oil Appearance Code**

| Code | Description Appearance               | Layer Thickness Interval (g/m <sup>2</sup> or µm) | Litres per km <sup>2</sup> |
|------|--------------------------------------|---|----------------------------|
| 1    | <i>Sheen (silvery/grey)</i>          | 0.04 – 0.30                                       | 40 – 300                   |
| 2    | <i>Rainbow</i>                       | 0.30 – 5.0  | 300 – 5,000                |
| 3    | <i>Metallic</i>                      | 5.0 – 50  | 5,000 – 50,000             |
| 4    | <i>Discontinuous True Oil Colour</i> | 50 – 200  | 50,000 – 200,000           |
| 5    | <i>Continuous True Oil Colour</i>    | 200 →   | 200,000 →                  |

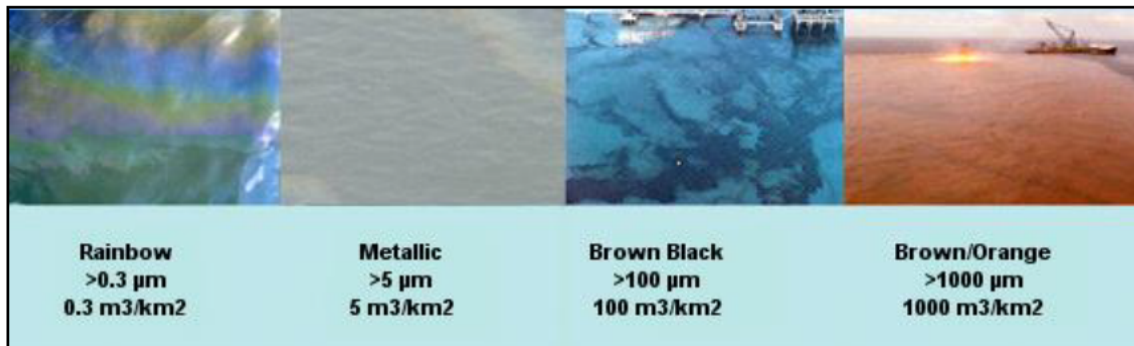


Figure 13 Photographs showing the difference between oil colour and thickness on the sea surface (source: adapted from OilSpillSolutions.org 2015)

Table 7 Thresholds used to classify the zones of sea surface exposure

| Oil concentration ( $\text{g}/\text{m}^2$ ) | Zone description |
|---|------------------|
| 0.5 - 10                                    | Low              |
| 10 - 25                                     | Moderate         |
| $> 25$                                      | High             |

## 6.2.2 Shoreline Contact Threshold

There are many different types of shorelines, ranging from cliffs, rocky beaches, sandy beaches, mud flats and mangroves, and each of these influences the volume of oil that can remain stranded ashore and its thickness before the shoreline saturation point occurs. For instance, a sandy beach may allow oil to percolate through the sand, thus increasing its ability to hold more oil ashore over tidal cycles and various wave actions than an equivalent area of water; hence oil can increase in thickness onshore over time. A sandy beach shoreline was assumed as the default shoreline type for the modelling herein, as it allows for the highest carrying capacity of oil (of the available open/exposed shoreline types). Hence the results contained herein would be indicative of a worst-case scenario, where the highest volume of oil may be stranded on the shoreline (when compared to other shoreline types, such as exposed rocky shores).

French et al. (1996) and French-McCay (2009) have defined an oil exposure threshold for shorebirds and wildlife (furbearing aquatic mammals and marine reptiles) on or along the shore at  $100 \text{ g}/\text{m}^2$ , which is based on studies for sub-lethal and lethal impacts. These thresholds have been used in previous environmental risk assessment studies (see French-McCay, 2003; French-McCay et al., 2004; French-McCay et al., 2011; NOAA, 2013). The  $100 \text{ g}/\text{m}^2$  threshold is also recommended in the Australian Maritime Safety Authority's (AMSA) foreshore assessment guide<sup>1</sup> as the acceptable minimum thickness that does not inhibit the potential for recovery and is best remediated by natural coastal processes alone (AMSA, 2007). The  $100 \text{ g}/\text{m}^2$  threshold has been selected to define the zone of potential moderate contact on the shorelines.

<sup>1</sup> Recommended for shoreline types including sandy beach, boulder shorelines, pebble shorelines, rock platforms and industry facility structures.

Observations by Lin and Mendelssohn (1996), demonstrated that loadings of more than 1,000 g/m<sup>2</sup> of oil during the growing season would be required to impact marsh plants significantly. Similar thresholds have been found in studies assessing oil impacts on mangroves (Grant et al., 1993; Suprayogi and Murray, 1999). The 1,000 g/m<sup>2</sup> threshold has been selected to define the zone of potential high contact on the shorelines.

Oil contact between 10 and 100 g/m<sup>2</sup> represents the socio-economic (or low contact) threshold.

The following thresholds (see Table 8) have therefore been derived to classify the shoreline contact.

**Table 8 Thresholds use to assess shoreline contact**

| Shoreline concentration (g/m <sup>2</sup> ) | Zone description |
|---|------------------|
| 10–100                                      | Low              |
| 100–1,000                                   | Moderate         |
| > 1,000                                     | High             |

### 6.2.3 Water Column Exposure Thresholds

Sub-surface exposure to submerged habitats is better represented by estimates for entrained or dissolved hydrocarbons in the water column.

Studies indicate that the dissolved aromatic compounds (typically the mono-aromatic hydrocarbons and the two and three ring poly-aromatic hydrocarbons) are commonly the largest contributor to the toxicity of solutions generated by mixing oil into water (Di Toro et al., 2007). The exposure level (threshold concentration over a given duration) was used to assess the potential for exposure to sub-sea habitats and species by rained and dissolved aromatic hydrocarbons. The threshold value for species toxicity in the water column is based on global data from French et al. (1999) and French-McCay (2002, 2003), which showed that species sensitivity (fish and invertebrates) to dissolved aromatics exposure > 4 days (96-hour LC<sub>50</sub>) under different environmental conditions varied from 6 to 400 µg/l (ppb) with an average of 50 ppb. This range covered 95% of aquatic organisms tested, which included species during sensitive life stages (eggs and larvae).

Based on scientific literature, a minimum threshold of 6 parts per billion (ppb) over 96-hours or equivalent was used to assess in-water low exposure zones (Engelhardt, 1983; Clark, 1984; Geraci and St. Aubin, 1988; Jenssen, 1994; Tsvetnenko, 1998). French-McCay, 2002 indicates that an average 96-hour LC<sub>50</sub> of 50 ppb and 400 ppb could serve as an acute lethal threshold to 5% and 50% to biota, respectively. Hence, the thresholds were used to represent the moderate and high exposure zones, respectively.

Given that the dissolved aromatics component of hydrocarbons in the water column are accounted for by the thresholds defined above, the environmental effects of the remaining undissolved hydrocarbons, essentially the entrained hydrocarbons in the water column, require different exposure thresholds.

Considering that entrained oil has undergone processes analogous to weathering and/or water-washing (i.e., many of the toxic soluble hydrocarbons have been removed through evaporation and/or dissolution), its toxicity is representative of true 'dispersed oil' phase impacts. OSPAR (2012) has published predicted no effect concentrations (PNEC) for 'dispersed oil' in produced formation water (PFW) discharges. Dispersed oil in PFW discharges are small, discrete droplets suspended in the discharged water which are very similar to insoluble dispersed oil droplets formed from subsea blowouts. In essence, the oil has been partitioned

(naturally separated) from gas/oil/water mixture by solubility (washing) and vapour pressure (evaporation) based on the individual hydrocarbon chemical properties.

The OSPAR PNEC for PFW is 70.5 ppb for protection of 95% of species, based on biomarker testing (i.e. whole organism responses) to total hydrocarbons (THC) by Smit et al., 2009. This PNEC represents an acceptable long term chronic exposure level from continuous point source discharges in the North Sea, which is one of the most concentrated areas in the world for oil and gas production.

Appropriate threshold values can be extrapolated from the NOECs examined in Smit et al., 2009 based on effects ranging from oxidative stress to impacts on growth, reproduction and survival and are represented by: 7 µg/l (7ppb) (for 1% affected fraction of species), 70.5µg/l (70ppb) (for 5% affected fraction of species) and 804 µg/l (804 ppb) (for 50% affected fraction of species).

Utilising methodologies contained in ANZECC (2000), which is based upon USEPA Guidelines, PNECs can be back-calculated to determine LC<sub>50</sub> values by applying a factor of 100 to the PNEC values. This approach is supported by assessment factor criteria contained within the European Chemicals Agency (2008) and the OECD Existing Chemicals Programme 2002 (OECD, 2002).

Considering the information above, the following conservative threshold values for entrained hydrocarbons are applied:

- PNEC (95% species protection): 70.5 µg/l (ppb) x 168 hours (chronic exposure)
- LC<sub>50</sub> (99% species protection): 700 µg/l (ppb) x 96 hours (acute exposure); and
- LC<sub>50</sub> (95% species protection): 7,050 µg/l (ppb) x 96 hours (acute exposure)

Table 9 and Table 10 provide a summary of the dissolved aromatic and entrained hydrocarbon threshold values used to define different levels of potential exposure in the modelling study.

**Table 9 Dissolved aromatic threshold values applied as part of the modelling study**

| Trigger level for dissolved aromatic concentrations (ppb) | Equivalent exposure of dissolved aromatics over 96 hrs (ppb.hrs) | Range of sensitive species potentially impacted from acute exposure | Potential level of exposure |
|---|--|---|-----------------------------|
| 6   | 576  | Very sensitive species  | Low                         |
| 50  | 4,800  | Average sensitive species   | Moderate                    |
| 400   | 38,400   | Tolerant sensitive species  | High                        |

**Table 10 Entrained hydrocarbon threshold values applied as part of the modelling study. Thresholds based on OSPAR guidelines**

| Trigger level for entrained hydrocarbon concentrations (ppb) | Equivalent exposure of entrained hydrocarbons (ppb.hrs) | Range of sensitive species potentially impacted from acute exposure | Potential level of exposure |
|--|---|---|-----------------------------|
| 70.5   | 11,844  | Very sensitive species  | Low                         |
| 700  | 67,200  | Very sensitive species  | Moderate                    |
| 7050   | 676,800   | Average sensitive species   | High                        |

### 6.3 Exposure Calculation

The thresholds used for the in-water concentrations of entrained hydrocarbons were described as an exposure over time, rather than an instantaneous peak value. The exposure is expressed as a concentration multiplied by the number of hours exposed at that concentration, in the units of parts per billion multiplied by hours (ppb.hrs).

There are two important and opposing mechanisms that will affect the cumulative exposure. The rate of uptake, due to the exposure concentration and the duration of exposure, and the rate of removal due to the ability of the organism to expel or metabolise hydrocarbons; a process referred to as depuration. Calculation for these natural removal processes are important so as to avoid falsely forecasting impacts by only allowing for the uptake of hydrocarbons, particularly over long duration release simulations.

The uptake of entrained hydrocarbons was calculated over time for each model grid cell by addition of the concentrations calculated at each subsequent time step, multiplied by the time interval (typically hourly). Depuration was calculated by applying an exponential decay function to the previously accumulated exposure.

A review of the literature describing the observed rates of depuration of hydrocarbons indicates that the reduction of concentration follows an exponential decay. For sub-lethal concentrations, depuration rates will be faster with increased concentration and then decrease as concentrations approach zero. Hence, depuration of the concentrations in a cell over each time step was calculated by applying an exponential decay function to the tissue concentration calculated by uptake.

Observed rates of depuration show significant variation for different soluble hydrocarbons and different organisms, varying from a few days to a few weeks (Solbakken et al., 1984). For this study, the decay coefficient was set so that the exposure would fall to 1% of an initial concentration over 1 week, given no further exposure.

Cumulative exposures at each time step were then compared to threshold exposures and any location where the exposure thresholds were ever exceeded during any simulation was mapped.

To illustrate the effect of allowing for depuration of hydrocarbons over time, an example time-series plot of concentration and exposure at a receptor location is presented in Figure 14. The time-series of concentration shows intermittent contacts to hydrocarbons with gaps between contacts, of the order of ~5 days. Such an outcome might be expected, for example, from variation in the position of hydrocarbon plumes resulting from variations in the current field during an ongoing discharge. The lower panel shows the calculated exposure if depuration is not considered (blue line) and the exposure where an exponential depuration rate is allowed for, assuming a time-scale of 7 days for tissue concentrations to reduce to 1% of a starting concentration.

In the case where depuration was ignored (blue line), the calculated exposure simply increases with addition of each hydrocarbon concentration, and remains constant during times where there is no contact to hydrocarbons. In the case where depuration is allowed for (green line), exposure decreases exponentially between exposures. The maximum exposure occurs around day 50, where there was a prolonged (~5 days) exposure to a high concentration. The threshold exposure is not exceeded by the intermittent exposures to low concentrations but is exceeded at around day 48 when higher concentrations occurred for a longer duration.

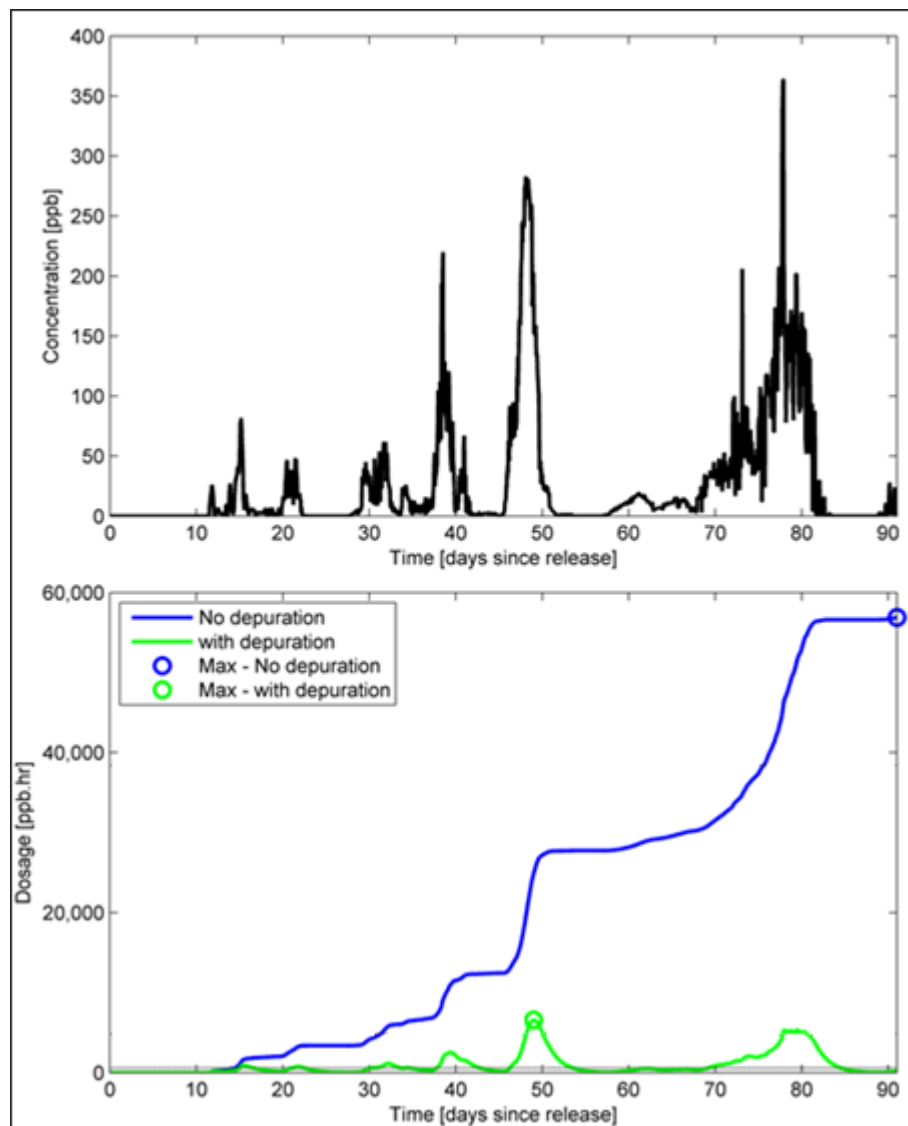


Figure 14 Example time series plot of concentration of entrained hydrocarbons (top) at a receptor, and exposure (bottom) with no depuration (blue) and with depuration (green)

## 6.4 Receptors Assessed

Shorelines were assessed for potential exposure to oil accumulation above specified thresholds. Figure 15 and Figure 16 present the marine parks, RAMSAR, reefs shoals and banks assessed for oil exposure above minimum threshold and shoreline contact from hydrocarbons.

Note, due to the number of biologically important areas in this region, individual maps for each species have been provided in Appendix A.

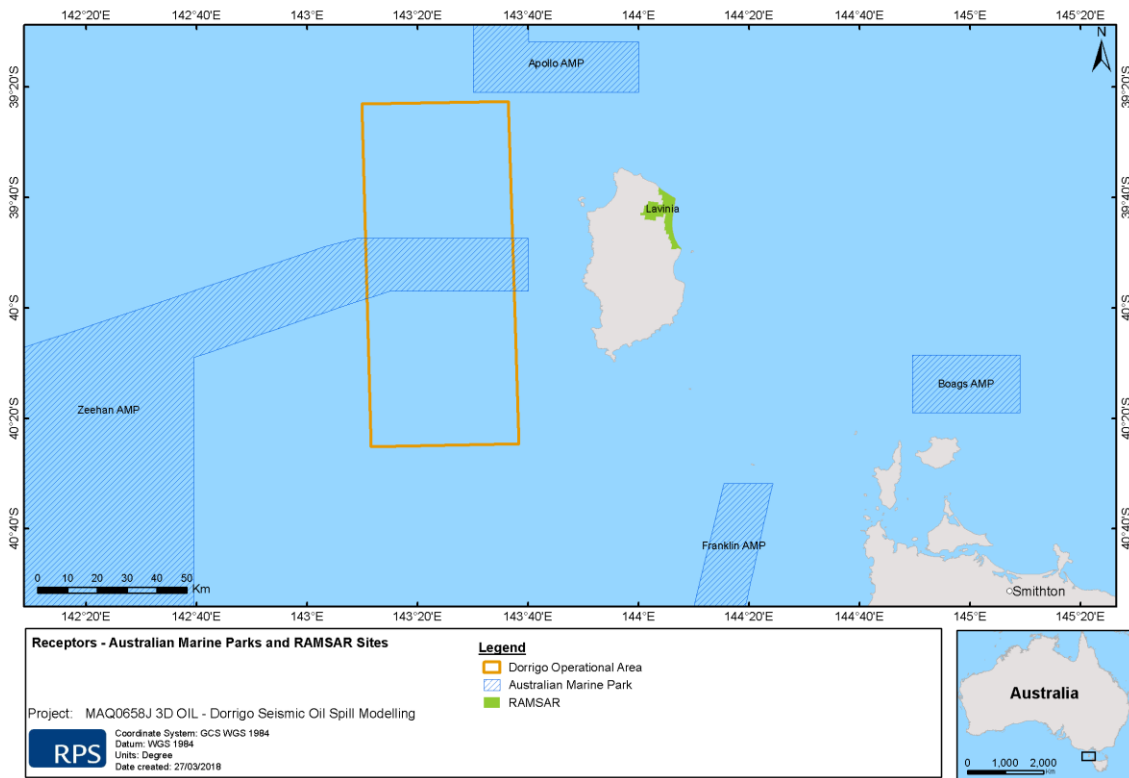


Figure 15 Marine parks and Ramsar sites assessed for oil exposure.

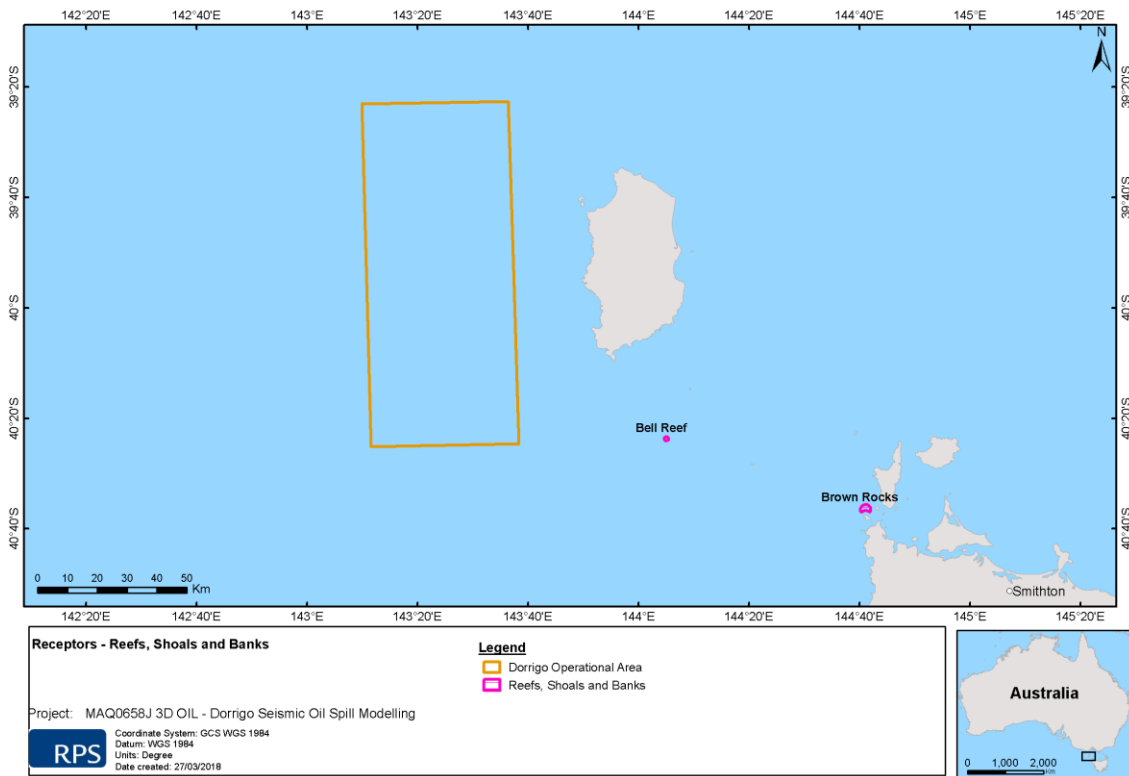


Figure 16 Reefs, shoals and banks assessed for oil exposure.

## 7 Oil Properties

The oil type used for the vessel collision incident was a marine diesel oil (MDO). It has a density of 829.1 kg/m<sup>3</sup> (API of 37.6), a pour point (-14°C) and a dynamic viscosity at 25°C of 4.0 cP, which indicates that this oil will spread quickly when spilt at sea and thin out to low thickness levels; which increases the rate of evaporation. The marine diesel has a strong tendency to entrain into the upper water column in the presence of moderate winds and breaking waves (>12 knots) but re-floats to the surface when the conditions calm, this process can delay the evaporation processes. Approximately, 5% (by mass) of the oil is considered “persistent hydrocarbons”. These oil properties categorise MDO as a Group 2 oil according to the International Tanker Owners Pollution Federation (ITOPF, 2014).

Table 11 and Table 12 show the physical characteristics and boiling point ranges for the MDO.

**Table 11 Physical characteristics.**

| <b>Characteristic</b>        | <b>Marine Diesel Oil</b> |
|------------------------------|--------------------------|
| Density (kg/m <sup>3</sup> ) | 829 @ 25°C               |
| API                          | 37.6                     |
| Dynamic viscosity (cP)       | 4 @ 25°C                 |
| Pour Point (°C)              | -14                      |
| Oil Property Category        | Group 2                  |

**Table 12 Boiling point ranges.**

| <b>Characteristic</b> | <b>Volatiles (%)</b>  | <b>Semi-volatiles (%)</b> | <b>Low volatiles (%)</b> | <b>Residual (%)</b> |
|-----------------------|-----------------------|---------------------------|--------------------------|---------------------|
| Boiling point (°C)    | <180                  | 180 – 265                 | 265 – 380                | >380                |
| Marine Diesel Oil     | 6.0                   | 34.6                      | 54.4                     | 5                   |
|                       | <i>Non-persistent</i> |                           |                          | <i>Persistent</i>   |

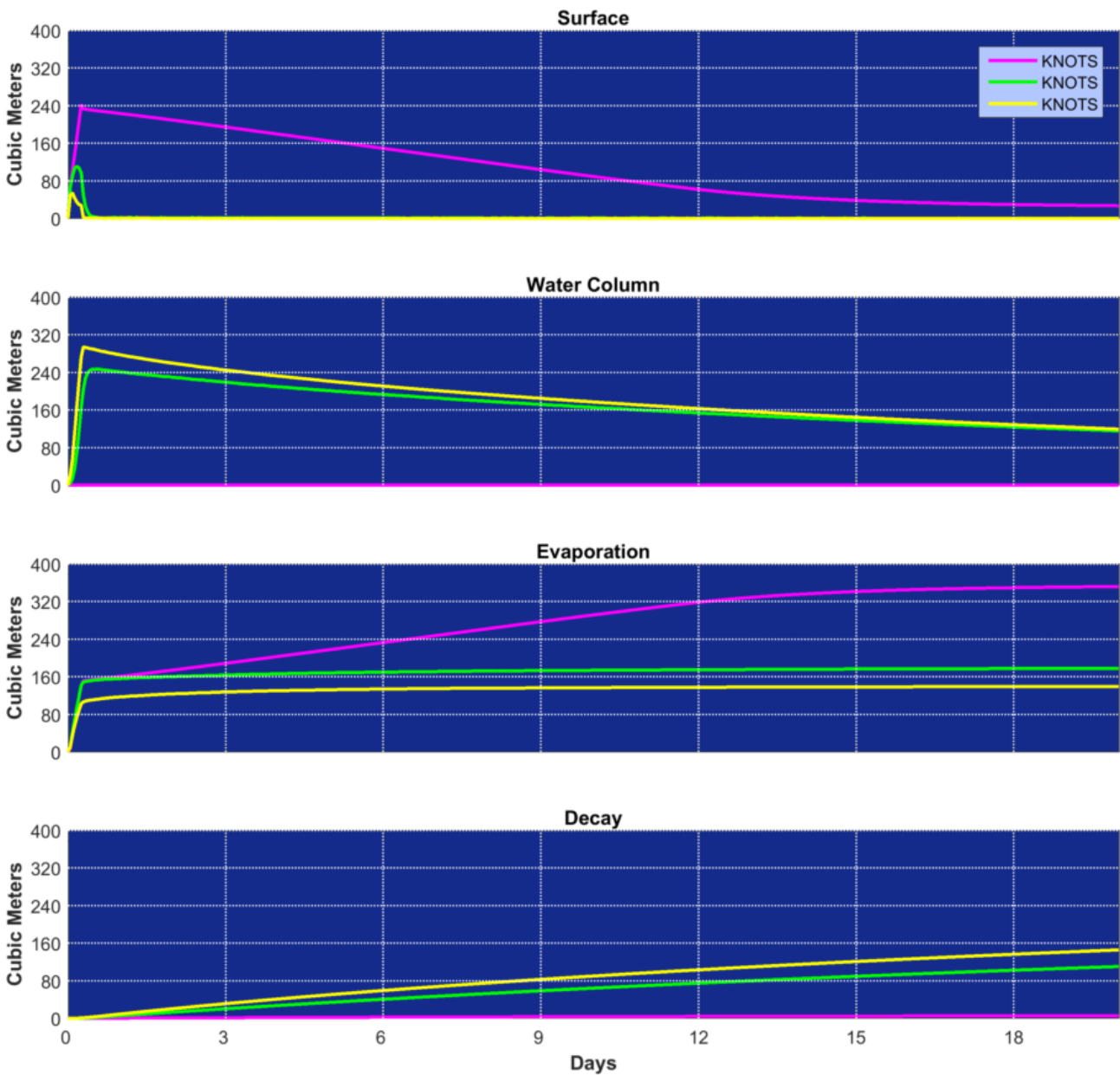


Figure 17 Weathering and fates graph, as a function of volume, under 5, 10 and 15 knot static wind conditions. Results are based on a 400 m<sup>3</sup> of MDO over 6 hours (tracked for 20 days).

## 8 Model Settings

Stochastic modelling was conducted to assess the risk and potential exposure to surrounding waters and contact to the shorelines throughout the proposed operational period following a hypothetical yet plausible scenario:

- A 400 m<sup>3</sup> surface release of marine diesel oil over 6 hours, to represent a vessel collision incident, from 100 randomly selected release sites within the permit area.

Table 13 provides a summary of the oil spill model settings and assumptions

**Table 13 Summary of the oil spill model settings used in this assessment.**

| Parameter   | Value  |
|---|--|
| Scenario description  | Vessel collision within the Dorigo marine seismic survey operational area  |
| Number of randomly selected spill start times                         | 100  |
| Model Period  | October to April   |
| Oil Type  | Marine Diesel Oil  |
| Spill Volume  | 400 m <sup>3</sup>   |
| Release Depth (m)   | Surface  |
| Release duration (hours)  | 6  |
| Simulation length (days)  | 20   |
| Surface oil concentration thresholds (g/m <sup>2</sup> )              | 0.5, 10 and 25   |
| Shoreline load threshold (g/m <sup>2</sup> )                          | 10, 100 and 1,000  |
| Dissolved aromatic dosages to assess the potential exposure (ppb.hrs) | 576 (6* ppb x 96 hrs, potential low exposure)<br>4,800 (50 ppb x 96 hrs, potential moderate exposure)<br>38,400 (400 ppb x 96 hrs, potential high exposure)            |
| Entrained oil dosages to assess the potential exposure (ppb.hrs)      | 11,844 (70.5 ppb x 168 hrs, potential low exposure)<br>67,200 (700 ppb x 96 hrs, potential moderate exposure)<br>676,800 (7,050 ppb x 96 hrs, potential high exposure) |

## 9 Interpreting Modelling Results

The results from the modelling study are presented in a number of tables and figures, which aim to provide an understanding of both the predicted sea surface exposure, shoreline contact and in-water exposure for the scenario.

The figures are based on the following principles:

- **The potential zones of exposure (surface oil, entrained hydrocarbons and dissolved aromatics)** – is determined by identifying the maximum loading (surface) or dosage (subsea) within a grid cell and is then classified according to identified surface or subsea thresholds.
- The **minimum time before oil exposure on the sea surface** – is determined by recording the elapsed time before sea surface exposure to a grid cell, at a specified threshold.
- The **probability of exposure/contact (surface oil, shoreline oil, entrained hydrocarbon or dissolved aromatic)** – is calculated by dividing the number of spill trajectories passing over that given cell (surface, shoreline or subsea) by the total number of spill trajectories, above the specified threshold value.
- **Maximum potential shoreline loading** – is determined by identifying the maximum loading within a shoreline cell and is then classified according to the identified thresholds (i.e. 100 g/m<sup>2</sup> and 1,000 g/m<sup>2</sup>).

The statistics are based on the following principles:

- The **greatest distance travelled by a spill trajectory** – is determined by: a) recording the maximum distance travelled by a single trajectory, within a scenario, from the release site to the identified exposure thresholds; and then b) report the greatest distance travelled by the **99<sup>th</sup> percentile spill trajectory (or second highest distance travelled by a single spill trajectory)**, along with the corresponding direction of travel from the release site.
- The **probability of shoreline contact** – is determined by recording to the number of spill trajectories to contact the shoreline, at a specific threshold, divided by the total number of spill trajectories within that scenario.
- The **minimum time before oil exposure** – is determined by recording the minimum time for a grid cell to record exposure, at a specific threshold.
- The **average volume of oil ashore for a single spill** – is determined by calculating the average volume of the all the single spill trajectories which were predicted to make shoreline contact within a scenario.
- The **maximum volume of oil ashore from a single spill trajectory** – is determined by identifying the single spill trajectory within a scenario/season, that recorded the maximum volume of oil to come ashore and presenting that value.
- The **average length of shoreline contacted by oil** - is determined by calculating the average of the length of shoreline (measured as grid cells) contacted by oil above a specified threshold.
- The **maximum length of shoreline contacted by oil** - is determined by recording the maximum length of shoreline (measured as grid cells) contacted by oil above a specified threshold.
- The **probability of oil exposure to a receptor** – is determined by recording the number of spill trajectories to reach a specified sea surface or subsea threshold within a receptor polygon, divided by the total number of spill trajectories within that scenario.

- The **minimum time before oil exposure to a receptor**– is determined by ranking the elapsed time before sea surface exposure, at a specified threshold, to grid cells within a receptor polygon and recording the minimum value.
- The **probability of oil contact to a receptor**– is determined by recording the number of spill trajectories to reach a specified shoreline contact threshold within a receptor polygon, divided by the total number of spill trajectories within that scenario.
- The **minimum time before shoreline contact to a receptor** – is determined by ranking the elapsed time before shoreline contact, at a specified threshold, to grid cells within a receptor polygon and recording the minimum value.
- The **average potential oil loading within a receptor** – is determined taking the average of the maximum loading to any grid cell within a polygon, for all simulations within a scenario/season, that recorded shoreline
- The **maximum potential oil loading within a receptor** – is determined by identifying the maximum loading to any grid cell within a receptor polygon, for a scenario.
- The **average volume of oil ashore within a receptor** – is determined by calculating the average volume of oil to come ashore within a receptor polygon, from all the single spill trajectories which were predicted to make shoreline contact within a scenario.
- The **maximum volume of oil ashore within a receptor** – is determined by recording the maximum volume of oil to come ashore within a receptor polygon, from all the single spill trajectories which were predicted to make shoreline contact within a scenario.
- The **average length of shoreline contacted within a receptor** is determined by calculating the average of the length of shoreline (measured as grid cells) contacted by oil within a receptor polygon, at a specified threshold, from all the single spill trajectories which were predicted to make shoreline contact within a scenario.
- The **maximum length of shoreline contacted by oil** is determined by recording the maximum length of shoreline (measured as grid cells) contacted by oil within a receptor polygon, at a specified threshold, from all the single spill trajectories which were predicted to make shoreline contact within a scenario

## 10 Results: 400m<sup>3</sup> Surface Release of MDO from a Vessel Collision within the Dorigo Marine Seismic Survey Area

This scenario examined a hypothetical release of 400 m<sup>3</sup> of MDO following a vessel collision within the Dorigo seismic survey area. 100 individual spill locations were randomly selected throughout the operation area to represent a hypothetical collision occurrence through multiple stages of the survey. A total of 100 spill trajectories were simulated and tracked for a period of 20 days.

Section 10.1 presents the potential exposure to the sea surface and shoreline contact, while Section 10.2 presents potential subsurface exposure.

For the modelling study each spill trajectory was tracked to the following minimum thresholds:

- Visible sea surface oil – 0.5 g/m<sup>2</sup>
- Shoreline oil contact – 10 g/m<sup>2</sup>
- Dissolved aromatics – 576 ppb.hrs
- Entrained hydrocarbons – 11,844 ppb.hrs

### 10.1 Sea Surface Exposure and Shoreline Contact

Table 14 details the maximum distance travelled by oil on the sea surface at each surface oil threshold. The maximum distance from a release site for potential of low, moderate and high exposure were 48 km (South) 14km (South) and 17km (East).

Table 15 provides a summary of shoreline contact at or above low threshold (10 g/m<sup>2</sup>). Modelling demonstrated a 2% probability of contact to any shoreline and an absolute minimum time for visible oil to come ashore of approximately 30 hours and had a maximum onshore volume of 30 m<sup>3</sup>.

Figure 18 illustrates zones of potential exposure on the sea surface for low (1–10 g/m<sup>2</sup>) moderate (10- 25 g/m<sup>2</sup>) and high (>25 g/m<sup>2</sup>) from October to April.

Figure 19 to Figure 21 demonstrate the probability of oil exposure on the sea surface above low, moderate and high exposure while Figure 22 to Figure 24 show the minimum amount of time before oil exposure reaches the sea surface.

Table 16 provides a summary of sea surface exposure to all receptors. Surface oil exposure was predicted to influence many Biologically Important Areas, due to the operational area overlapping these regions.

A summary of shoreline contact to individual receptors is outlined in Table 17. King Island was the only shoreline shown to be impacted, with a 2% probability and a peak volume of 30 m<sup>3</sup> onshore across a maximum length of 8 km.

Table 14 Summary of potential zones of sea surface exposure at each surface oil threshold.

| Period           | Distance and direction               | Zones of potential sea surface exposure |                                       |                                 |
|------------------|--------------------------------------|---|---------------------------------------|---------------------------------|
|                  |                                      | Low<br>(0.5–10 g/m <sup>2</sup> )       | Moderate<br>(10–25 g/m <sup>2</sup> ) | High<br>(>25 g/m <sup>2</sup> ) |
| October to April | Max. distance from release site (km) | 48                                      | 14                                    | 6                               |
|                  | Direction                            | South                                   | South                                 | South                           |

Table 15 Summary of shoreline contact across all shorelines

| Shoreline statistics   | October to April |
|--|------------------|
| Probability of contact to any shoreline (%)                  | 2                |
| Absolute minimum time for visible oil to shore (hours)       | 30               |
| Maximum volume of hydrocarbons ashore (m <sup>3</sup> )      | 30               |
| Average volume of hydrocarbons ashore (m <sup>3</sup> )      | 23               |
| Maximum length of the shoreline at 10 g/m <sup>2</sup> (km)  | 8                |
| Average shoreline length (km) at 10 g/m <sup>2</sup> (km)    | 5                |
| Maximum length of the shoreline at 100 g/m <sup>2</sup> (km) | 6                |
| Average length of the shoreline at 100 g/m <sup>2</sup> (km) | 4                |
| Maximum shoreline length at 1,000 g/m <sup>2</sup> (km)      | 0                |
| Average shoreline length at 1,000 g/m <sup>2</sup> (km)      | 0                |

Table 16 Summary of the potential sea surface exposure to receptors from October to April.

| Receptor                                  | Probability of oil exposure on the sea surface (%) |                                    |                              | Minimum time before oil exposure on the sea surface (hours) |                                    |                              |
|---|--|------------------------------------|------------------------------|---|------------------------------------|------------------------------|
|   | Low (0.5–10 g/m <sup>2</sup> )                     | Moderate (10–25 g/m <sup>2</sup> ) | High (>25 g/m <sup>2</sup> ) | Low (0.5–10 g/m <sup>2</sup> )                              | Moderate (10–25 g/m <sup>2</sup> ) | High (>25 g/m <sup>2</sup> ) |
| King Island                               | 2  | 0                                  | 0                            | 30  | -                                  | -                            |
| Tasmania State Waters                     | 3  | 0                                  | 0                            | 30  | -                                  | -                            |
| Australian Exclusive Economic Zone        | 100  | 100                                | 65                           | <1  | <1                                 | <1                           |
| Apollo AMP                                | 2  | 0                                  | 0                            | 20  | -                                  | -                            |
| Zeehan AMP                                | 20   | 15                                 | 6                            | <1  | <1                                 | <1                           |
| West Tasmania Canyons                     | 17   | 6                                  | 4                            | <1  | <1                                 | <1                           |
| Antipodean Albatross - Foraging           | 100  | 100                                | 65                           | <1  | <1                                 | <1                           |
| Black-browed Albatross - Foraging         | 100  | 100                                | 65                           | <1  | <1                                 | <1                           |
| Black-faced Cormorant - Foraging          | 3  | 0                                  | 0                            | 30  | -                                  | -                            |
| Bullers Albatross - Foraging              | 100  | 100                                | 65                           | <1  | <1                                 | <1                           |
| Campbell Albatross - Foraging             | 100  | 100                                | 65                           | <1  | <1                                 | <1                           |
| Indian Yellow-nosed Albatross - Foraging  | 100  | 100                                | 65                           | <1  | <1                                 | <1                           |
| Little Penguin - Foraging                 | 3  | 0                                  | 0                            | 30  | -                                  | -                            |
| Short-tailed Shearwater - Foraging        | 100  | 100                                | 65                           | <1  | <1                                 | <1                           |
| Shy Albatross - Foraging                  | 100  | 100                                | 65                           | <1  | <1                                 | <1                           |
| Wedge-tailed Shearwater - Foraging        | 65   | 64                                 | 41                           | <1  | <1                                 | <1                           |
| Wandering Albatross - Foraging            | 100  | 100                                | 65                           | <1  | <1                                 | <1                           |
| White Shark - Distribution                | 100  | 100                                | 65                           | <1  | <1                                 | <1                           |
| White-faced Storm-petrel - Foraging       | 28   | 16                                 | 11                           | <1  | <1                                 | <1                           |
| Common Diving-petrel - Foraging           | 100  | 100                                | 65                           | <1  | <1                                 | <1                           |
| Pygmy Blue Whale - Foraging               | 98   | 95                                 | 62                           | <1  | <1                                 | <1                           |
| Southern Right Whale - Migration          | 90   | 88                                 | 57                           | <1  | <1                                 | <1                           |
| Southern Right Whale - Connecting Habitat | 2  | 0                                  | 0                            | 30  | -                                  | -                            |
| Pygmy Blue Whale - Distribution           | 91   | 89                                 | 58                           | <1  | <1                                 | <1                           |

Table 17 Summary of shoreline contact to individual shoreline receptors.

| Shoreline Receptor | Maximum probability of shoreline loading (%) |                       |                         | Minimum time before shoreline accumulation (hours) |                       |                         | Load on shoreline (g/m <sup>2</sup> ) |      | Volume on shoreline (m <sup>3</sup> ) |      | Mean length of shoreline contacted (km) |                       |                         | Maximum length of shoreline contacted (km) |                       |                         | Minimum time before visible sea surface exposure (hours) |
|--------------------|--|-----------------------|-------------------------|--|-----------------------|-------------------------|---------------------------------------|------|---------------------------------------|------|---|-----------------------|-------------------------|--|-----------------------|-------------------------|--|
|                    | >10 g/m <sup>2</sup>                         | >100 g/m <sup>2</sup> | >1,000 g/m <sup>2</sup> | >10 g/m <sup>2</sup>                               | >100 g/m <sup>2</sup> | >1,000 g/m <sup>2</sup> | Mean                                  | Peak | Mean                                  | Peak | >10 g/m <sup>2</sup>                    | >100 g/m <sup>2</sup> | >1,000 g/m <sup>2</sup> | >10 g/m <sup>2</sup>                       | >100 g/m <sup>2</sup> | >1,000 g/m <sup>2</sup> |  |
| King Island        | 2  | 2                     | 0                       | 30   | 39                    | -                       | 404                                   | 912  | 23                                    | 30   | 5                                       | 4                     | 0                       | 8  | 6                     | 0                       | 30   |

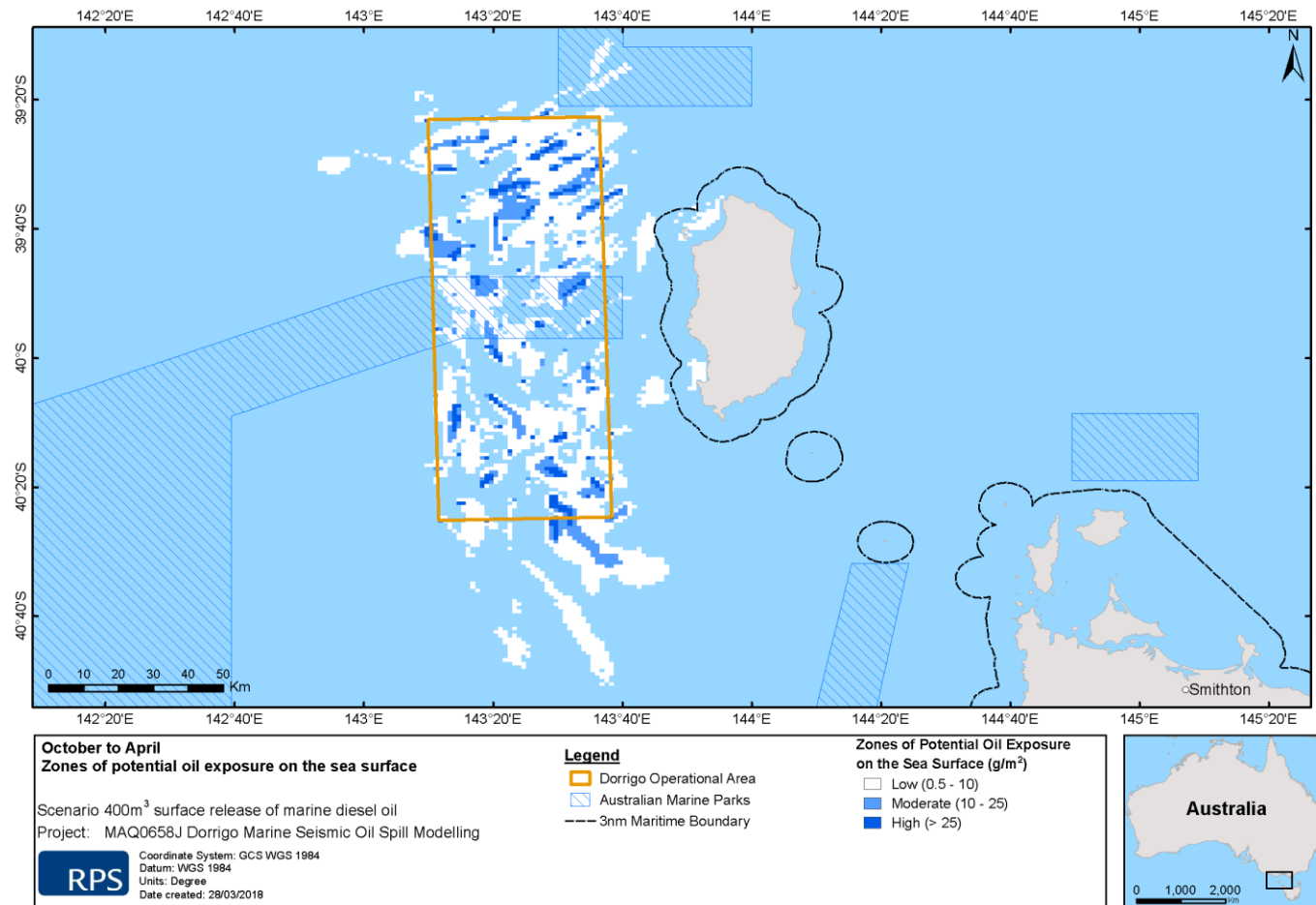


Figure 18 Zones of potential exposure on the sea surface.

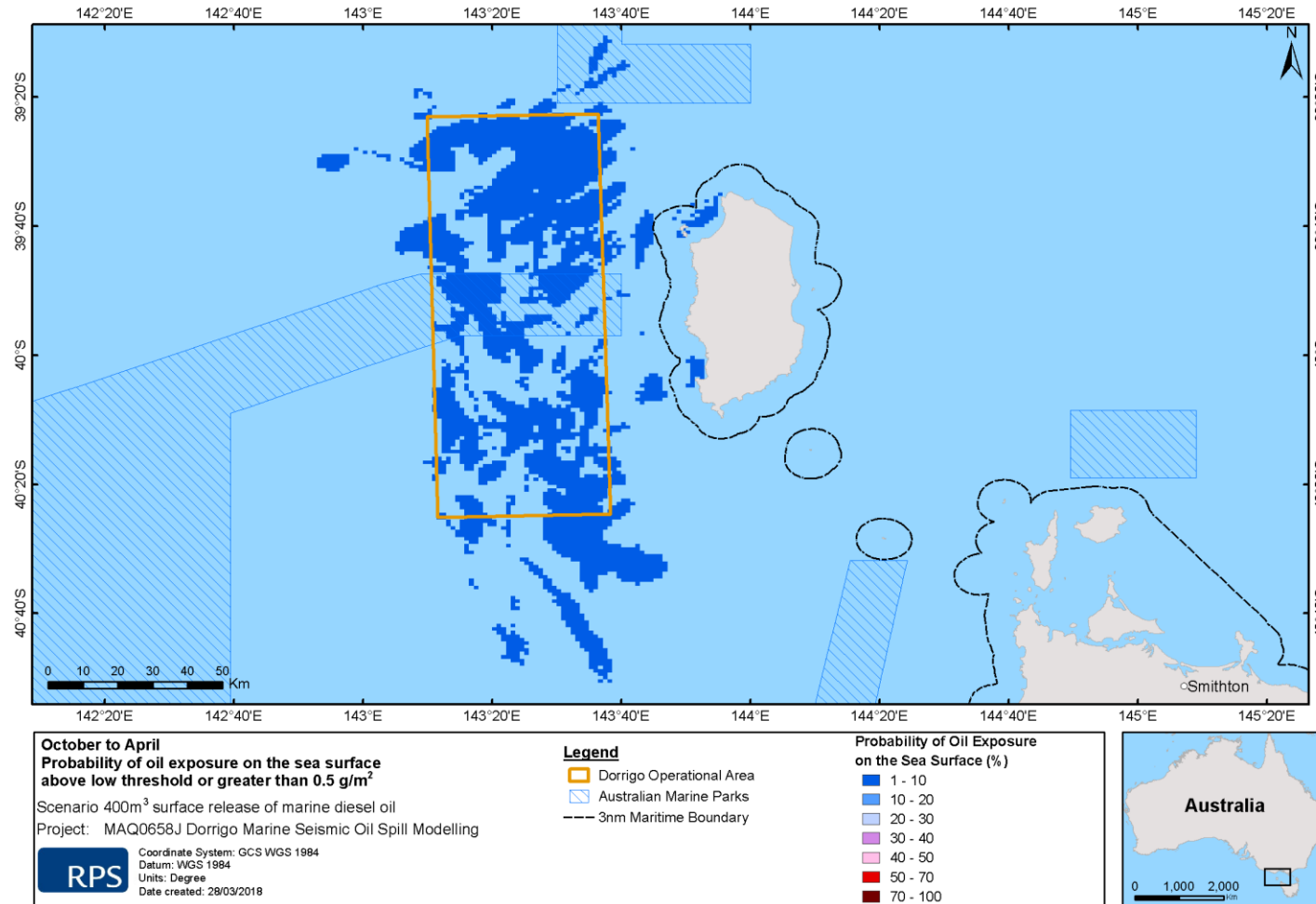


Figure 19 Probability of oil exposure on the sea surface above low exposure ( $\geq 1 \text{ g/m}^2$ ).

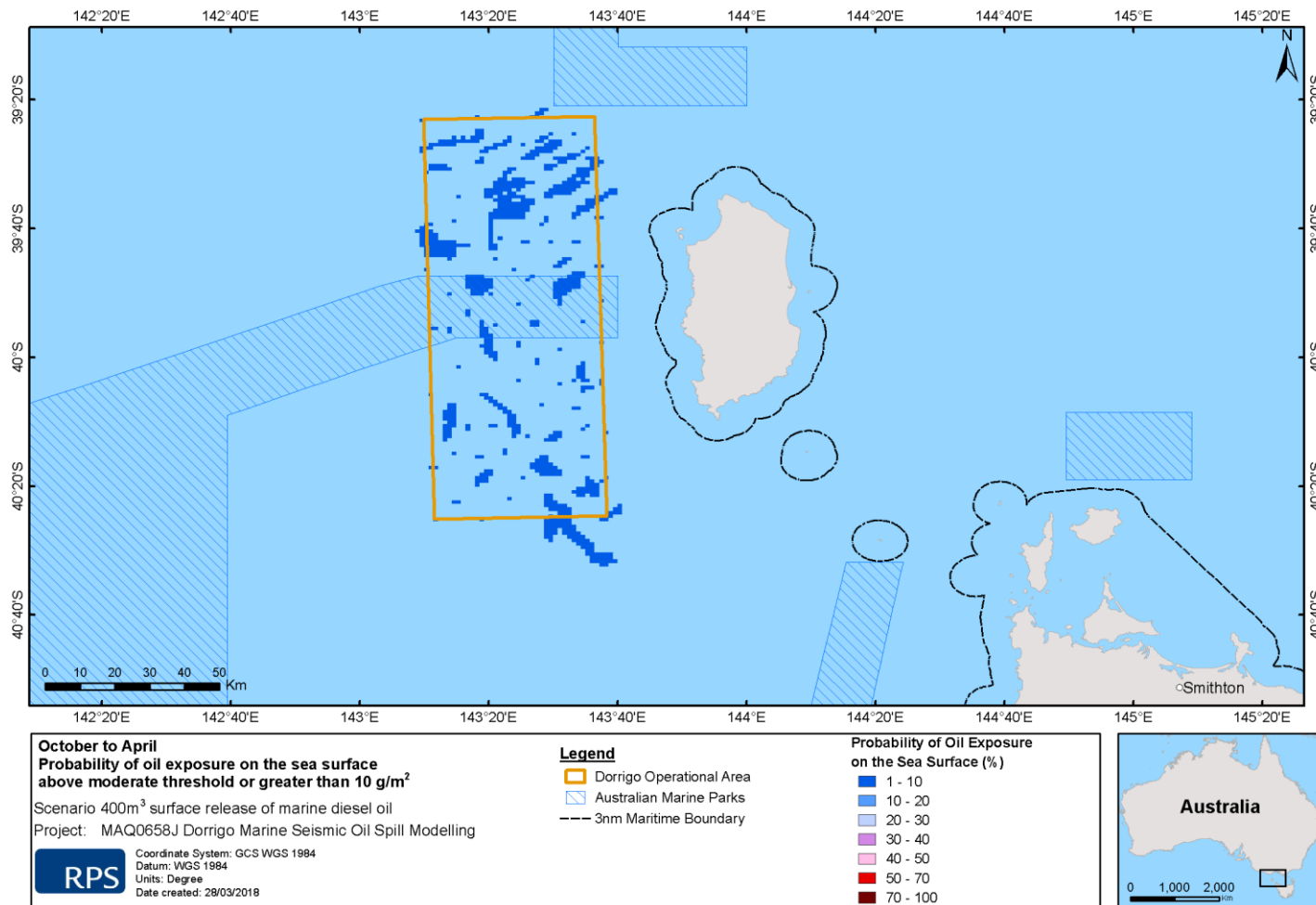


Figure 20 Probability of oil exposure on the sea surface above moderate exposure (≥10 g/m<sup>2</sup>).

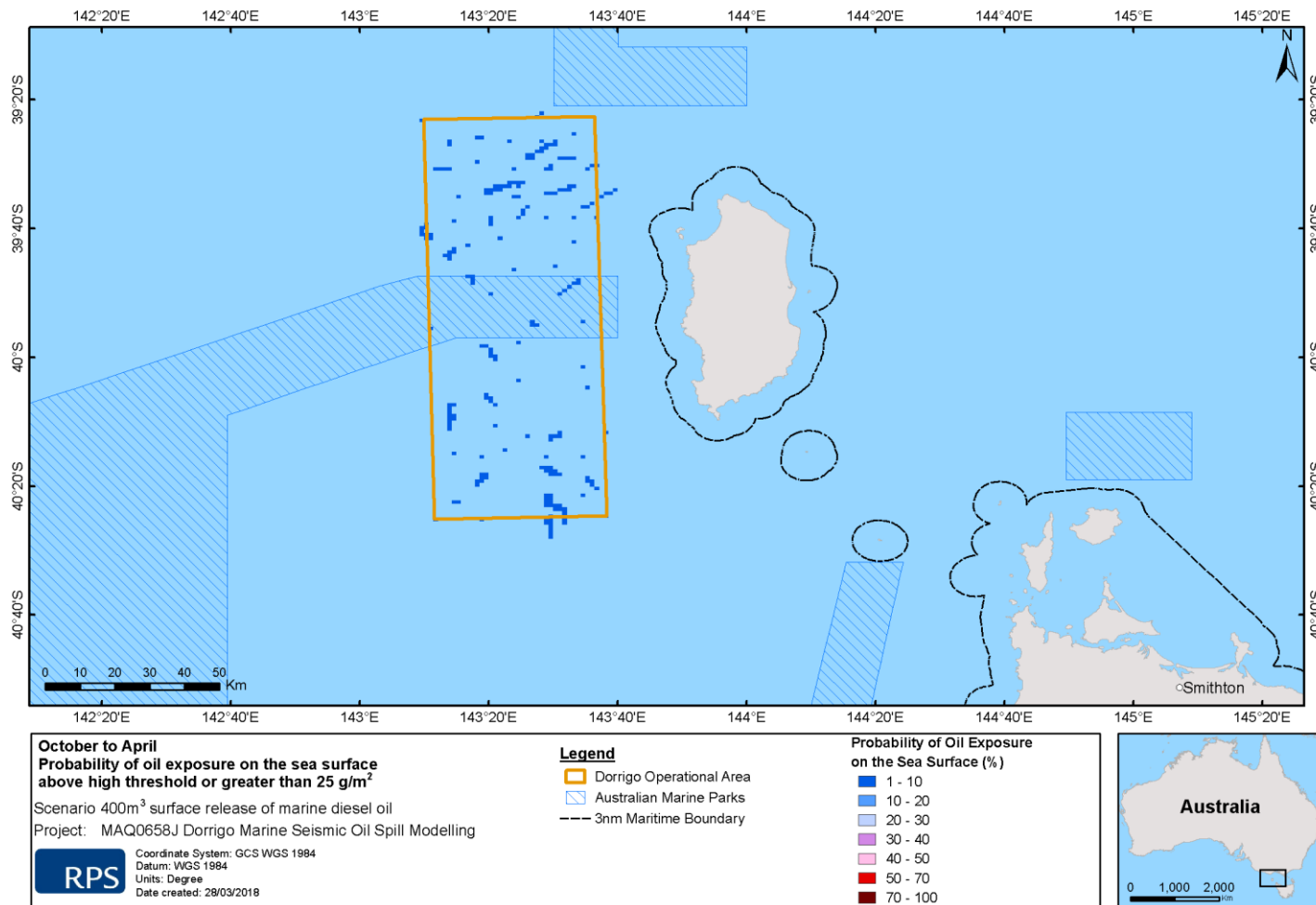


Figure 21 Probability of oil exposure on the sea surface above high exposure ( $\geq 25 \text{ g/m}^2$ ).

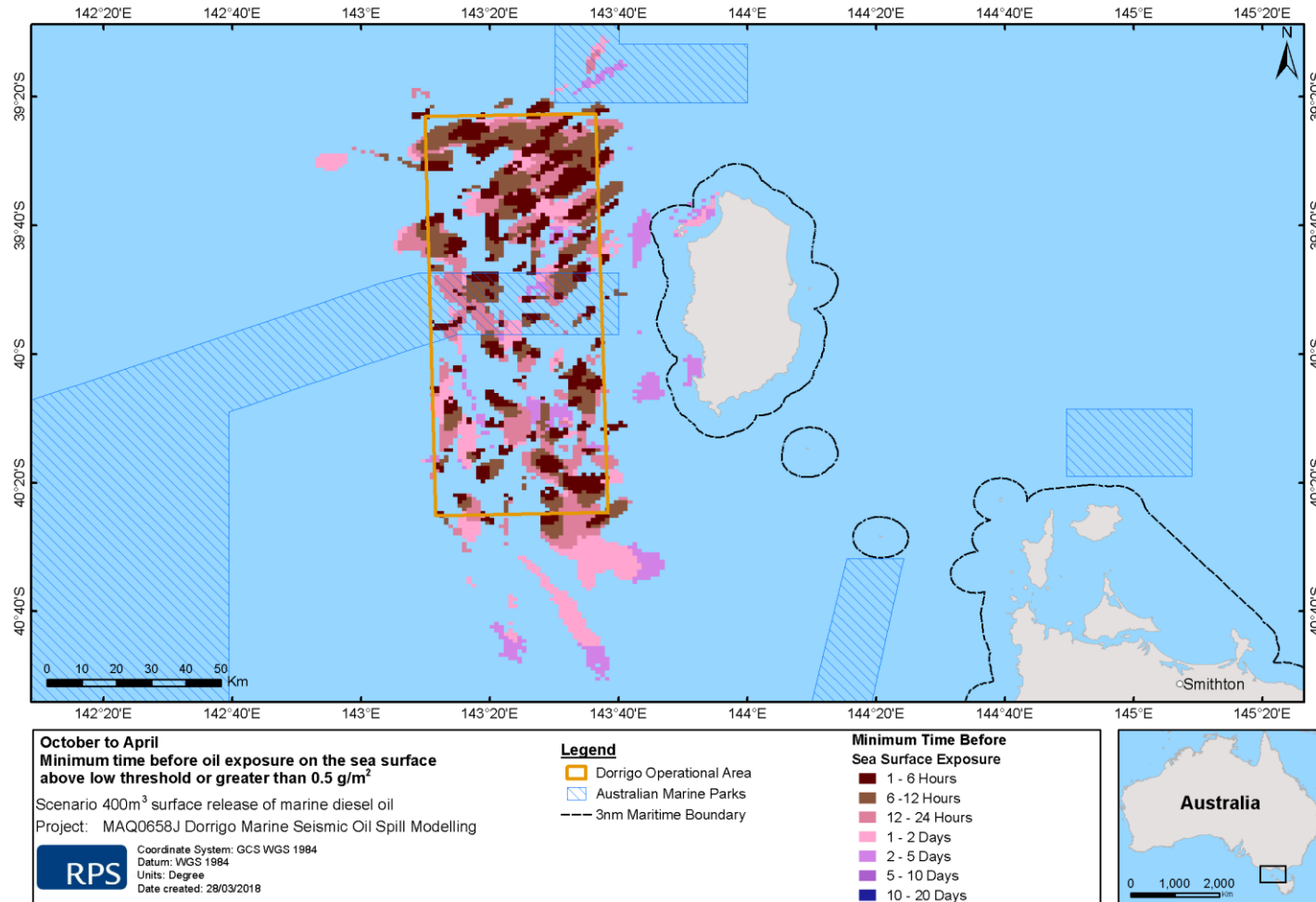


Figure 22 Minimum time before oil exposure on the sea surface above low exposure ( $\geq 0.5 \text{ g/m}^2$ ).

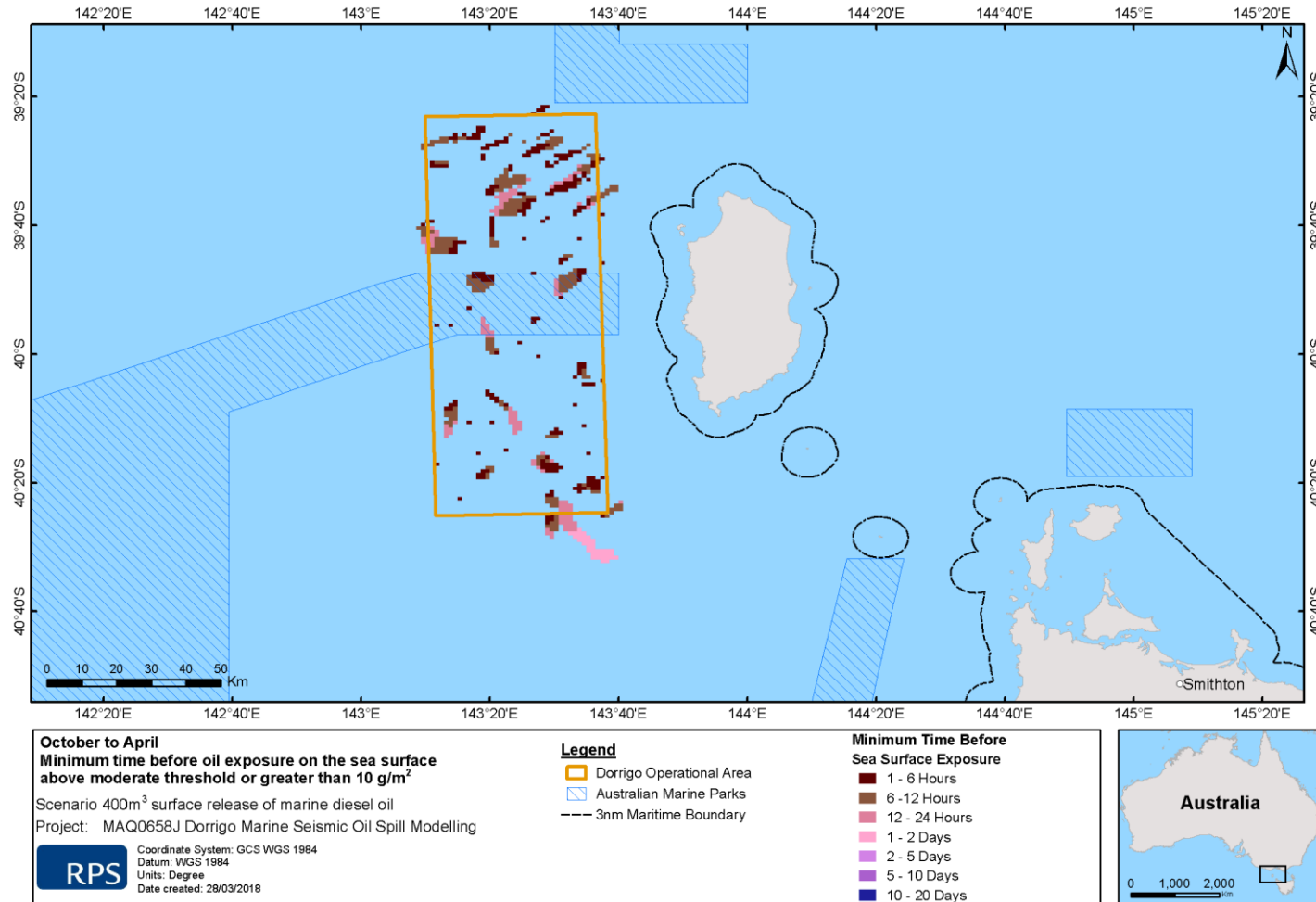


Figure 23 Minimum time before oil exposure on the sea surface above moderate exposure (≥10 g/m<sup>2</sup>).

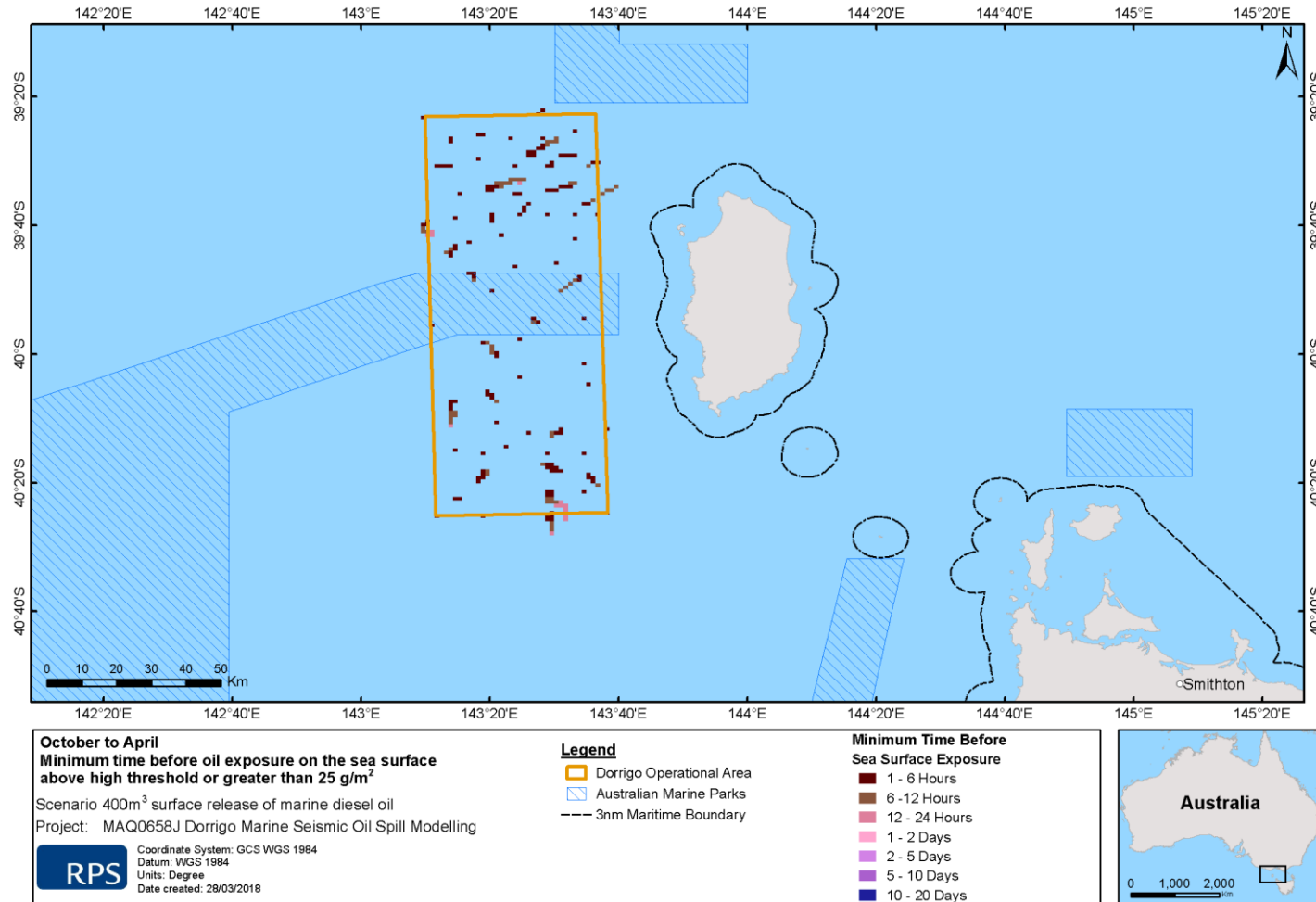


Figure 24 Minimum time before oil exposure on the sea surface above high exposure ( $\geq 25 \text{ g/m}^2$ ).

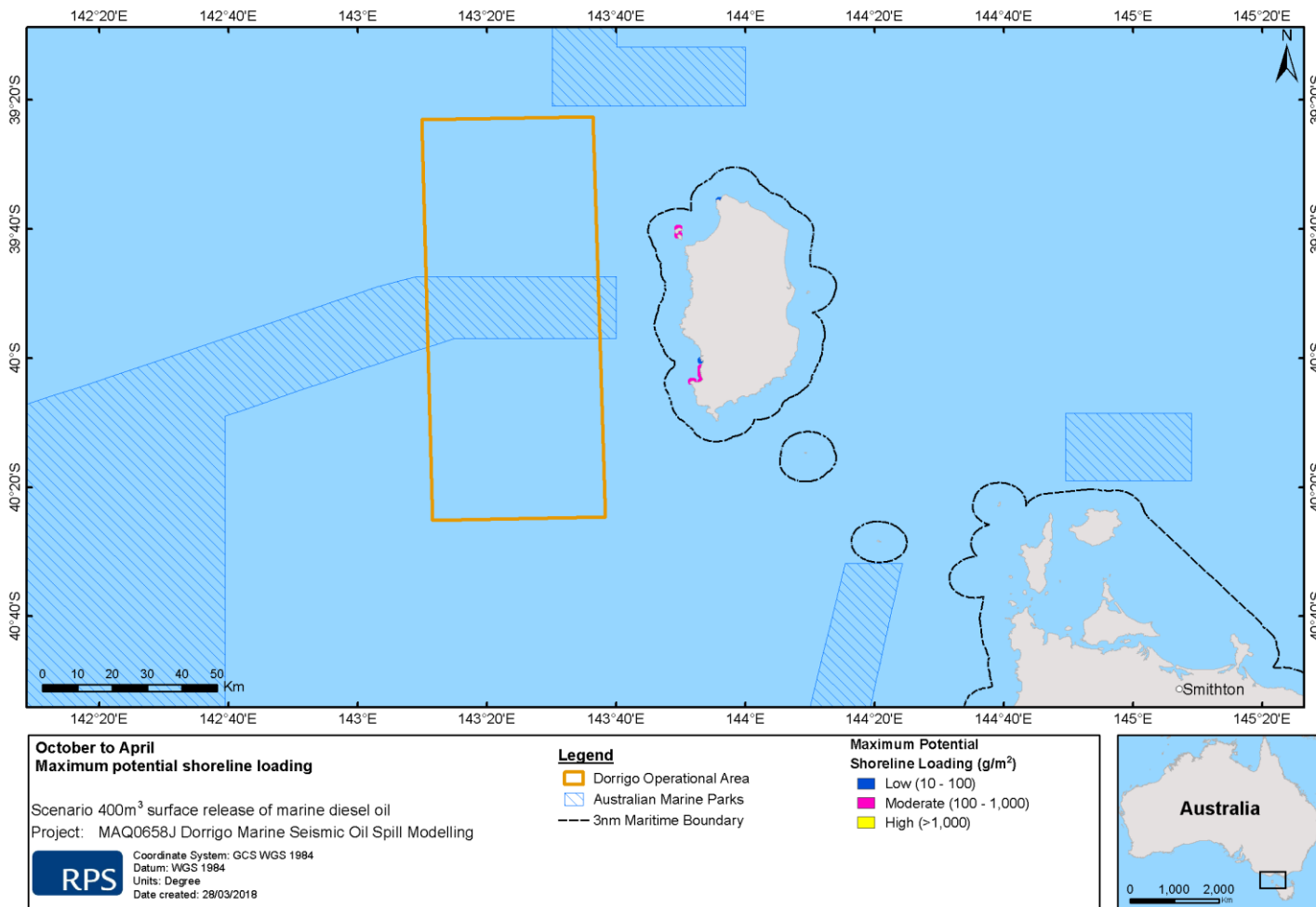


Figure 25 Maximum potential shoreline loading from October to April.

## 10.2 Subsurface Exposure

### 10.2.1 Dissolved Aromatics

No zones of exposure to dissolved aromatics above the low exposure thresholds of 576 ppb.hrs were observed.

### 10.2.2 Entrained Hydrocarbons

Table 18 summarises the potential receptors impacted by entrained hydrocarbons and the probability of at low (>11,844 ) moderate (>67,200 ppb.hrs) and high (>676,800 ppb.hrs) thresholds in the 0 – 10m depth layer

Low level of entrained hydrocarbons is shown to occasionally impact on bird foraging areas including 6 species of albatross, 2 species of shearwater and 2 species of petrel.

No zones of exposure to entrained hydrocarbons were observed at or above the moderate exposure threshold of 67,200 ppb.hrs, under any of the environmental conditions or depth profiles assessed

**Table 18 Maximum exposure to entrained hydrocarbons and sea surface probability.**

| Receptor                                 | Maximum exposure to entrained hydrocarbons (ppb.hrs) | Probability of exposure to entrained hydrocarbons (%) |                           |                        |
|--|--|---|---------------------------|------------------------|
|  |  | Low (11,844 ppb.hrs)                                  | Moderate (67,200 ppb.hrs) | High (676,800 ppb.hrs) |
| King Island                              | 12,154   | 1   | 0                         | 0                      |
| Tasmania State Waters                    | 12,154   | 1   | 0                         | 0                      |
| Australian Exclusive Economic Zone       | 52,186   | 2   | 0                         | 0                      |
| Apollo AMP                               | 13,844   | 1   | 0                         | 0                      |
| Zeehan AMP                               | 35,947   | 2   | 0                         | 0                      |
| West Tasmania Canyons                    | 52,186   | 1   | 0                         | 0                      |
| Antipodean Albatross - Foraging          | 52,186   | 2   | 0                         | 0                      |
| Black-browed Albatross - Foraging        | 52,186   | 2   | 0                         | 0                      |
| Black-faced Cormorant - Foraging         | 12,154   | 1   | 0                         | 0                      |
| Bullers Albatross - Foraging             | 52,186   | 2   | 0                         | 0                      |
| Campbell Albatross - Foraging            | 52,186   | 2   | 0                         | 0                      |
| Indian Yellow-nosed Albatross - Foraging | 52,186   | 2   | 0                         | 0                      |
| Little Penguin - Foraging                | 12,154   | 1   | 0                         | 0                      |
| Short-tailed Shearwater - Foraging       | 52,186   | 2   | 0                         | 0                      |
| Shy Albatross - Foraging                 | 52,186   | 2   | 0                         | 0                      |
| Wedge-tailed Shearwater - Foraging       | 41,663   | 2   | 0                         | 0                      |
| Wandering Albatross - Foraging           | 52,186   | 2   | 0                         | 0                      |
| White Shark - Distribution               | 52,186   | 2   | 0                         | 0                      |
| White-faced Storm-petrel - Foraging      | 23,069   | 1   | 0                         | 0                      |
| Common Diving-petrel - Foraging          | 52,186   | 2   | 0                         | 0                      |
| Pygmy Blue Whale - Foraging              | 41,663   | 2   | 0                         | 0                      |

RPS

## 11 References

- American Society for Testing and Materials (ASTM) 2013. F2067-13 Standard Practice for Development and Use of Oil-Spill Trajectory Models, ASTM International, West Conshohocken (PA).
- Australian Maritime Safety Authority (AMSA) 2007, 'Foreshore Assessment, Termination of Clean-up and Rehabilitation Monitoring', viewed 12 February 2014, [https://www.amsa.gov.au/environment/maritime-environmental-emergencies/national-plan/ESC/documents/Foreshore\\_Assessment\\_and\\_Termination.pdf](https://www.amsa.gov.au/environment/maritime-environmental-emergencies/national-plan/ESC/documents/Foreshore_Assessment_and_Termination.pdf)
- Australian Maritime Safety Authority (AMSA) 2012, 'Australian Maritime Safety Authority Technical Guideline for the Preparation of Marine Pollution Contingency Plans for Marine and Coastal Facilities Australian Maritime Safety Authority', viewed 15 January 2015, [https://www.amsa.gov.au/forms-and-publications/Publications/AMSA413\\_Contingency\\_Planning\\_Guidelines.pdf](https://www.amsa.gov.au/forms-and-publications/Publications/AMSA413_Contingency_Planning_Guidelines.pdf)
- Andersen, OB 1995, 'Global ocean tides from ERS 1 and TOPEX/POSEIDON altimetry', *Journal of Geophysical Research: Oceans*, vol. 100, no. C12, pp. 25249–25259.
- Australian and New Zealand Environment and Conservation Council (ANZECC), 2000. Australian and New Zealand guidelines for fresh and marine water quality. Volume 1, The guidelines (National water quality management strategy; no.4). Australian and New Zealand Environment and Conservation Council, Agriculture and Resource Management Council of Australia and New Zealand.
- Bonn Agreement 2009, Bonn Agreement aerial operations handbook, 2009 - Publication of the Bonn Agreement, London, viewed 13 January 2015, [http://www.bonnagreement.org/site/assets/files/3947/ba-ao\\_h\\_revision\\_2\\_april\\_2012.pdf](http://www.bonnagreement.org/site/assets/files/3947/ba-ao_h_revision_2_april_2012.pdf)
- Chassignet, EP, Hurlburt, HE, Smedstad, OM, Halliwell, GR, Hogan, PJ, Wallcraft, AJ, Baraille, R & Bleck, R 2007, 'The HYCOM (hybrid coordinate ocean model) data assimilative system', *Journal of Marine Systems*, vol. 65, no. 1, pp. 60–83.
- Chassignet, E, Hurlburt, H, Metzger, E, Smedstad, O, Cummings, J & Halliwell, G 2009, 'U.S. GODAE: Global Ocean Prediction with the HYbrid Coordinate Ocean Model (HYCOM)', *Oceanography*, vol. 22, no. 2, pp. 64–75.
- Clark, RB, 1984 'Impact of oil pollution on seabirds', *Environmental Pollution*, vol. 33, no.1, pp. 1–22.
- Condie, SA., & Andrewartha, JR (2008). Circulation and connectivity on the Australian Northwest Shelf. *Continental Shelf Research*, 28, 1724-1739.
- Davies, AM 1977a, 'The numerical solutions of the three-dimensional hydrodynamic equations using a B-spline representation of the vertical current profile', in JC Nihoul (ed), *Bottom Turbulence: Proceedings of the 8<sup>th</sup> Liège Colloquium on Ocean Hydrodynamics*, Elsevier Scientific, Amsterdam, pp. 1–25.
- Davies, AM 1977b, 'Three-dimensional model with depth-varying eddy viscosity', in JC Nihoul (ed), *Bottom Turbulence: Proceedings of the 8<sup>th</sup> Liège Colloquium on Ocean Hydrodynamics*, Elsevier Scientific, Amsterdam, pp. 27–48.
- DEWHA, 2007. Characterisation of the marine environment in the north marine region. Marine Division, Department of the environment, water heritage and the arts.
- DEWHA. 2008. The North-West Marine Bioregional Plan - Bioregional Profile. Retrieved February 12, 2013, from Australian Government Department of Environment, Water, Heritage and the Arts: <http://www.environment.gov.au/coasts/mbp/publications/north-west/pubs/bioregional-profile.pdf>
- Di Toro, DM, McGrath, JA & Stubblefield, WA 2007, 'Predicting the toxicity of neat and weathered crude oil: Toxic potential and the toxicity of saturated mixtures', *Environmental Toxicology and Chemistry*, vol. 26, no. 1, pp. 24–36.
- Engelhardt, FR 1983, 'Petroleum effects on marine mammals', *Aquatic Toxicology*, vol. 4, no.3, pp. 199–217.
- European Chemicals Agency. (2008). Chapter R.10 - Characterisation of dose [concentration] -response for environment. In *Guidance on information requirements and chemical safety assessment* (pp. 26-29). ECHA.
- French, D, Reed, M, Jayko, K, Feng, S, Rines, H, Pavignano, S, Isaji, T, Puckett, S, Keller, A, French III, FW, Gifford, D, McCue, J, Brown, G, MacDonald, E, Quirk, J, Natzke, S, Bishop, R, Welsh, M, Phillips, M, Ingram, BS 1996, *The CERCLA Type A natural resource damage assessment model for coastal and marine environments*

- (NRDAM/CME), Technical Documentation, Volume I - Model Description, Final Report, Office of Environmental Policy and Compliance, U.S. Department of the Interior, Washington DC.
- French, D, Schuttenberg, H & Isaji, T 1999, 'Probabilities of oil exceeding thresholds of concern: examples from an evaluation for Florida Power and Light', Proceedings of the 22<sup>nd</sup> Arctic and Marine Oil Spill Program (AMOP) Technical Seminar, Environment Canada, Alberta, pp. 243–270.
- French-McCay, DP 2002, 'Development and application of an oil toxicity and exposure model, OilToxEx', Environmental Toxicology and Chemistry, vol. 21, no. 10, pp. 2080-2094.
- French-McCay, DP 2003, 'Development and application of damage assessment modelling: example assessment for the North Cape oil spill', Marine Pollution Bulletin, vol. 47, no. 9, pp. 9–12.
- French-McCay, DP 2004, 'Spill impact modelling: development and validation', Environmental Toxicology and Chemistry, vol. 23, no.10, pp. 2441–2456.
- French-McCay, DP 2009, 'State-of-the-art and research needs for oil spill impact assessment modelling', Proceedings of the 32<sup>nd</sup> Arctic and Marine Oil Spill Program (AMOP) Technical Seminar, Environment Canada, Ottawa, pp. 601–653.
- French-McCay, D, Rowe, JJ, Whittier, N, Sankaranarayanan, S, & Etkin, DS 2004, 'Estimate of potential impacts and natural resource damages of oil', Journal of Hazardous Materials, vol. 107, no. 1, pp. 11–25.
- French-McCay, D, Reich, D, Rowe, J, Schroeder, M & Graham, E 2011, 'Oil spill modeling input to the offshore environmental cost model (OECM) for US-BOEMRE's spill risk and costs evaluations', Proceedings of the 34<sup>th</sup> Arctic and Marine Oil Spill Program (AMOP) Technical Seminar, Environment Canada, Ottawa.
- French-McCay, D, Jayko, K, Li, Z, Horn, M, Kim, Y, Isaji, T, Crowley, D, Spaulding, M, Decker, L, Turner, C, Zamorski, S, Fontenault, J, Schmmkier, R & Rowe, J 2015, 'Technical Reports for Deepwater Horizon Water Column Injury Assessment: WC\_TR.14: Modeling Oil Fate and Exposure Concentrations in the Deepwater Plume and Rising Oil Resulting from the Deepwater Horizon Oil Spill' RPS ASA, South Kingston, Rhode Island.
- French-McCay, D, Li, Z, Horn, M, Crowley, D, Spaulding, ML & Turner, C 2016, 'Modeling oil fate and subsurface exposure concentrations from the Deepwater Horizon oil spill', Proceedings of the 39<sup>th</sup> Arctic and Marine Oil Spill Program (AMOP) Technical Seminar, Environment and Climate Change Canada, Ottawa
- Geraci, JR., & St. Aubin, DJ 1988, Synthesis of effects of oil on marine mammals. 292. Ventura, CA, USA: US Department of the Interior, Minerals Management Service, Atlantic OCS Region, OCS Study, MMS 880049.
- Gordon, R 1982, 'Wind driven circulation in Narragansett Bay' PhD thesis, Department of Ocean Engineering, University of Rhode Island.
- Grant, DL, Clarke, PJ & Allaway, WG 1993, 'The response of grey mangrove (*Avicennia marina* (Forsk.) Vierh) seedlings to spills of crude oil,' The Journal of Experimental Marine Biological Ecology, vol. 171, no. 2, pp. 273–295.
- Isaji, T & Spaulding, M 1984, 'A model of the tidally induced residual circulation in the Gulf of Maine and Georges Bank', Journal of Physical Oceanography, vol. 14, no. 6, pp. 1119–1126.
- Isaji, T, Howlett, E, Dalton C, & Anderson, E 2001, 'Stepwise-continuous-variable-rectangular grid hydrodynamics model', Proceedings of the 24<sup>th</sup> Arctic and Marine Oil spill Program (AMOP) Technical Seminar (including 18<sup>th</sup> TSOCS and 3<sup>rd</sup> PHYTO), Environment Canada, Edmonton, pp. 597–610.
- International Tankers Owners Pollution Federation (ITOPF) 2014. Technical Information Paper 2 -Fate of Marine Oil Spills, International Tankers Owners Pollution Federation td, UK.
- Jenssen, BM 1994, 'Review article: Effects of Oil Pollution, Chemically Treated Oil, and Cleaning on the Thermal Balance of Birds', Environmental Pollution, vol.86, no. 2, pp. 207–215.
- Koops, W, Jak, RG & van der Veen, DPC 2004, 'Use of dispersants in oil spill response to minimise environmental damage to birds and aquatic organisms', Proceedings of the Interspill 2004: Conference and Exhibition on Oil Spill Technology, Trondheim, presentation 429.
- Kostianoy, AG, Ginzburg, AI, Lebedev, SA, Frankignoulle, M & Delille, B 2003, 'Fronts and mesoscale variability in the southern Indian Ocean as inferred from the TOPEX/POSEIDON and ERS-2 Altimetry data', Oceanology, vol. 43, no. 5, pp. 632–642.
- Levitus, S, Antonov, JI, Baranova, OK, Boyer, TP, Coleman, CL, Garcia, HE, Grodsky, AI, Johnson, DR, Locarnini, RA, Mishonov, AV, Reagan, JR, Sazama, CL, Seidov, D, Smolyar, I, Yarosh, ES & Zweng, MM 2013, 'The World Ocean Database', Data Science Journal, vol.12, no. 0, pp. WDS229–WDS234.

- Li, Z, Spaulding, M, French-McCay, D, Crowley, D & Payne JR 2017, 'Development of a unified oil droplet size distribution model with application to surface breaking waves and subsea blowout releases considering dispersant effects', *Marine Pollution Bulletin*, vol. 114, no. 1, pp 247–257.
- Li, Z, Spaulding, M & French-McCay, D, 'An algorithm for modeling entrainment and naturally and chemically dispersed oil droplet size distribution under surface breaking wave conditions', *Marine Pollution Bulletin*, In Press.
- Lin, Q & Mendelssohn, IA 1996, 'A comparative investigation of the effects of south Louisiana crude oil on the vegetation of fresh, brackish and Salt Marshes', *Marine Pollution Bulletin*, vol. 32, no. 2, pp. 202–209.
- Ludicone, D, Santoleri, R, Marullo, S & Gerosa, P 1998, 'Sea level variability and surface eddy statistics in the Mediterranean Sea from TOPEX/POSEIDON data. *Journal of Geophysical Research*, vol. 103, no. C2, pp. 2995–3011.
- Matsumoto, K, Takanezawa, T & Ooe, M 2000, 'Ocean tide models developed by assimilating TOPEX/POSEIDON altimeter data into hydrodynamical model: A global model and a regional model around Japan', *Journal of Oceanography*, vol. 56, no.5, pp. 567–581.
- National Oceanic and Atmospheric Administration (NOAA) 2013, Screening level risk assessment package Gulf state, Office of National Marine Sanctuaries & Office of Response and Restoration, Washington DC.
- The Organisation for Economic Co-operation and Development (OECD) 2002, Chapter 4: Initial Assessment of Data. In OECD, Manual for Investigation of HPV Chemicals, pp. 1-11.
- Oil Spill Solutions 2015, Evaluation - The Theory of Oil Slick Appearances, viewed 6 January 2015, <http://www.oilspillsolutions.org/evaluation.htm>
- OSPAR Commission (OSPAR) 2012, OSPAR guidelines in support of recommendation 2012/5 for risk-based approach to the management of produced water discharges from offshore installations. OSPAR Commission, p. 21.
- Owen, A 1980, 'A three-dimensional model of the Bristol Channel', *Journal of Physical Oceanography*, vol. 10, pp. 1290–1302.
- Qiu, B & Chen, S 2010, 'Eddy-mean flow interaction in the decadal modulating Kuroshio Extension system', *Deep-Sea Research II*, vol. 57, no. 13, pp. 1098–1110.
- Saha, S, Moorthi, S, Pan, H-L, Wu, X, Wang, J & Nadiga, S 2010, 'The NCEP Climate Forecast System Reanalysis', *Bulletin of the American Meteorological Society*, vol. 91, no. 8, pp. 1015–1057.
- Scholten, MCTH, Kaag, NHBM, Dokkum, HP van, Jak, R.G., Schobben, HPM & Slob, W 1996, Toxische effecten van olie in het aquatische milieu, TNO report TNO-MEP – R96/230, Den Helder.
- Smit, MG, Bechmann, RK, Hendriks, AJ, Skadsheim, A, Larsen, BK, Baussant, T, Shaw, B & Sanni, S 2009, 'Relating biomarkers to whole-organism effects using species sensitivity distributions: A pilot study for marine species exposed to oil', *Environmental Toxicology and Chemistry*, vol. 28, no. 5, pp. 1104-1109.
- Spaulding, ML., Kolluru, VS, Anderson, E & Howlett, E 1994, 'Application of three-dimensional oil spill model (WOSM/OILMAP) to hindcast the Braer Spill', *Spill Science and Technology Bulletin*, vol. 1, no. 1, pp. 23–35.
- Solbakken, JE, Ingebrigtsen, K & Palmork, KH 1984, 'Comparative study on the fates of the polychlorinated biphenyl 2, 4, 5, 20, 40, 50-hexachlorobiphenyl and the polycyclic aromatic hydrocarbon phenanthrene in flounder (*Platichthys flesus*) determined by scintillation counting and autoradiography', *Marine Biology*, vol. 83, pp. 239-246.
- Suprayogi, B & Murray, F 1999, 'A field experiment of the physical and chemical effects of two oils on mangroves', *Environmental and Experimental Botany*, vol. 42, no. 3, pp. 221–229.
- Tsvetnenko, Y 1998, 'Derivation of Australian tropical marine water quality criteria for protection of aquatic life from adverse effects of petroleum hydrocarbons', *Environmental Toxicology and Water Quality*, vol.13, no. 4, pp. 273–284.
- Willmott, CJ 1981, 'On the validation of models', *Physical Geography*, vol. 2, no. 2, pp.184–194.
- Willmott, CJ 1982, 'Some comments on the evaluation of model performance', *Bulletin of the American Meteorological Society*, vol. 63, no. 11, pp.1309–1313.
- Willmott CJ, Ackleson SG, Davis RE, Feddema JJ, Klink, KM, Legates, DR, O'Donnell, J & Rowe, CM 1985, 'Statistics for the evaluation of model performance', *Journal of Geophysical Research*, vol. I 90, no. C5, pp. 8995–9005.
- Willmott, CJ & Matsuura, K 2005, 'Advantages of the mean absolute error (MAE) over the root mean square error (RMSE) in assessing average model performance', *Journal of Climate Research*, vol. 30, no. 1, pp. 79–82.



Yaremchuk, M & Tangdong, Q 2004, 'Seasonal variability of the large-scale currents near the coast of the Philippines', *Journal of Physical Oceanography*, vol. 34, no., 4, pp. 844–855.

Zigic, S, Zapata, M, Isaji, T, King, B, & Lemckert, C 2003, *Modelling of Moreton Bay using an ocean/coastal circulation model*, Auckland, NZ: Proceedings of the Coasts and Ports Australasian Conference.

# Appendix A

## Biologically Important Areas

---

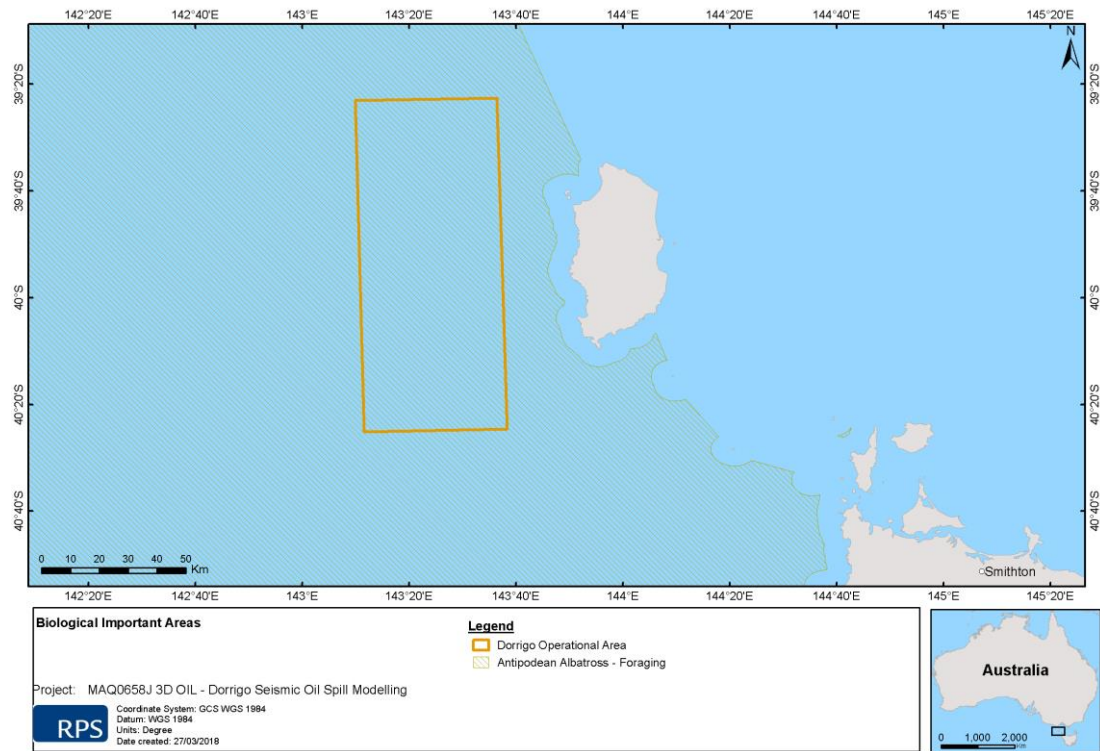


Figure 26 Biologically important areas for the antipodean albatross assessed for oil exposure.

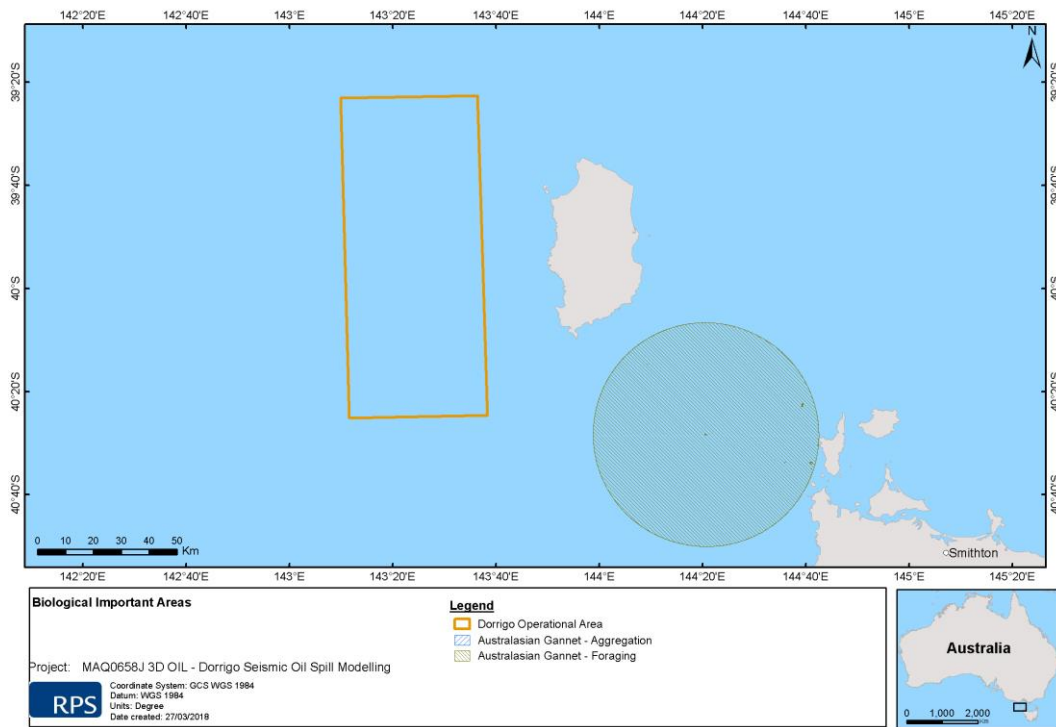


Figure 27 Biologically important areas for the australasian gannet assessed for oil exposure

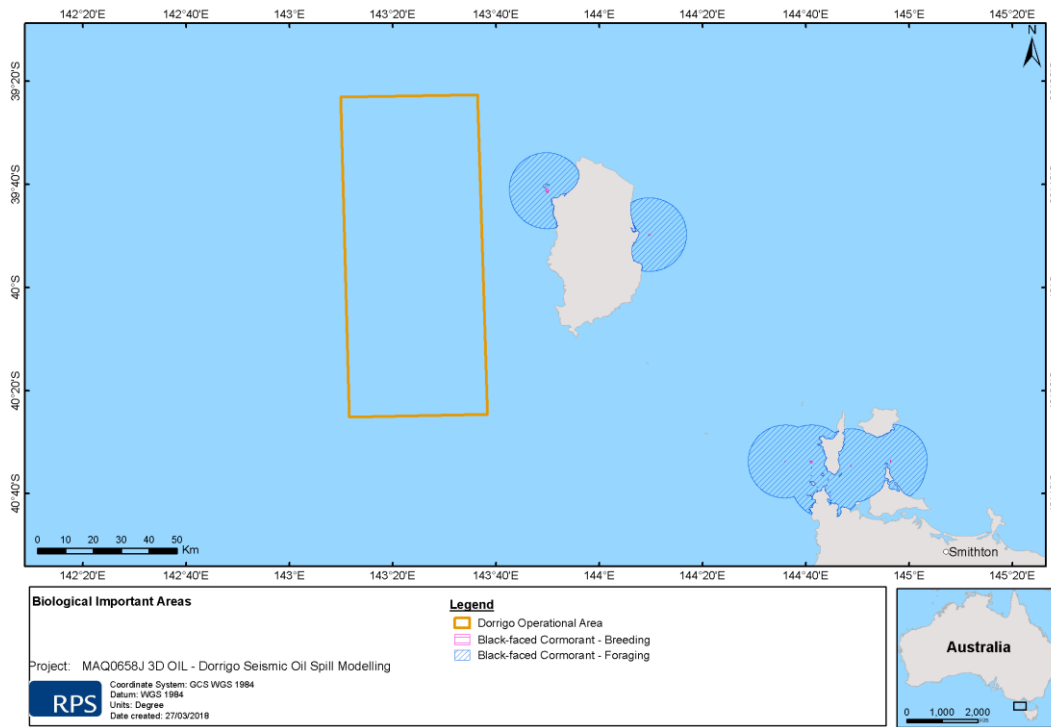


Figure 28 Biologically important areas for the black-faced cormorant assessed for oil exposure

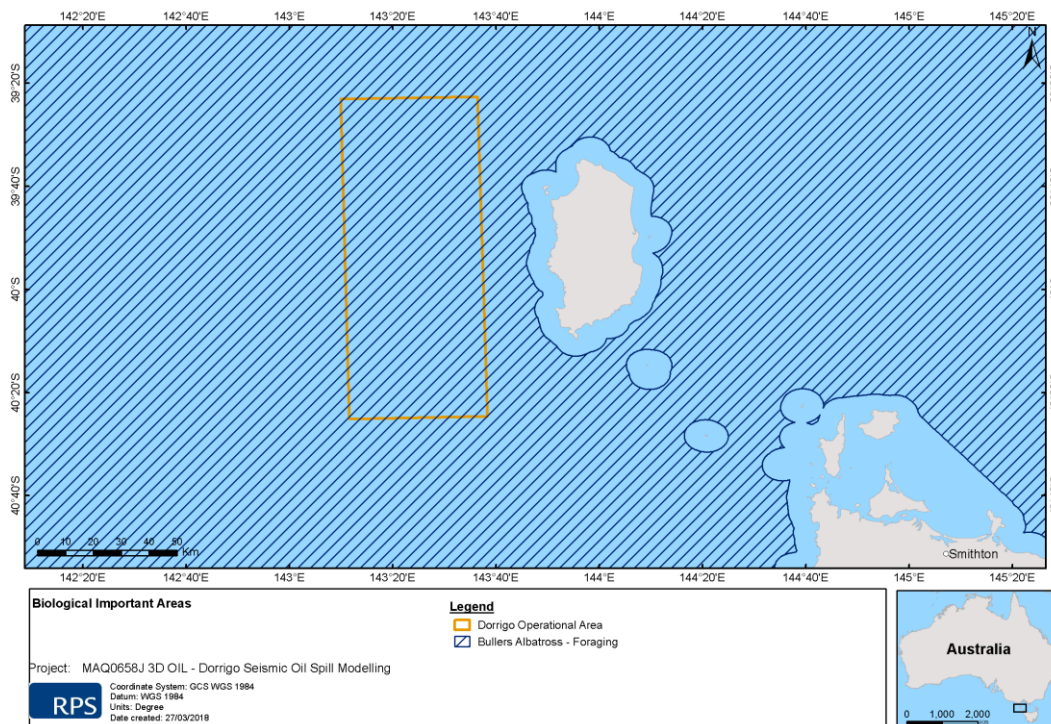


Figure 29 Biologically important areas for the buller's albatross assessed for oil exposure.

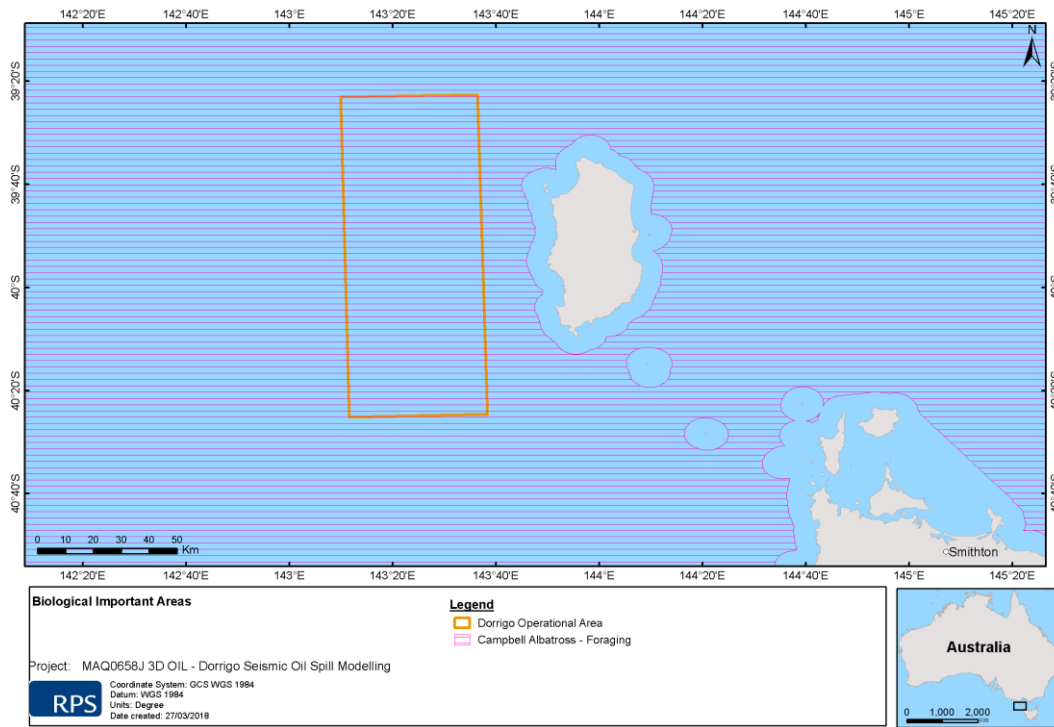


Figure 30 Biologically important areas for the campbell albatross assessed for oil exposure.

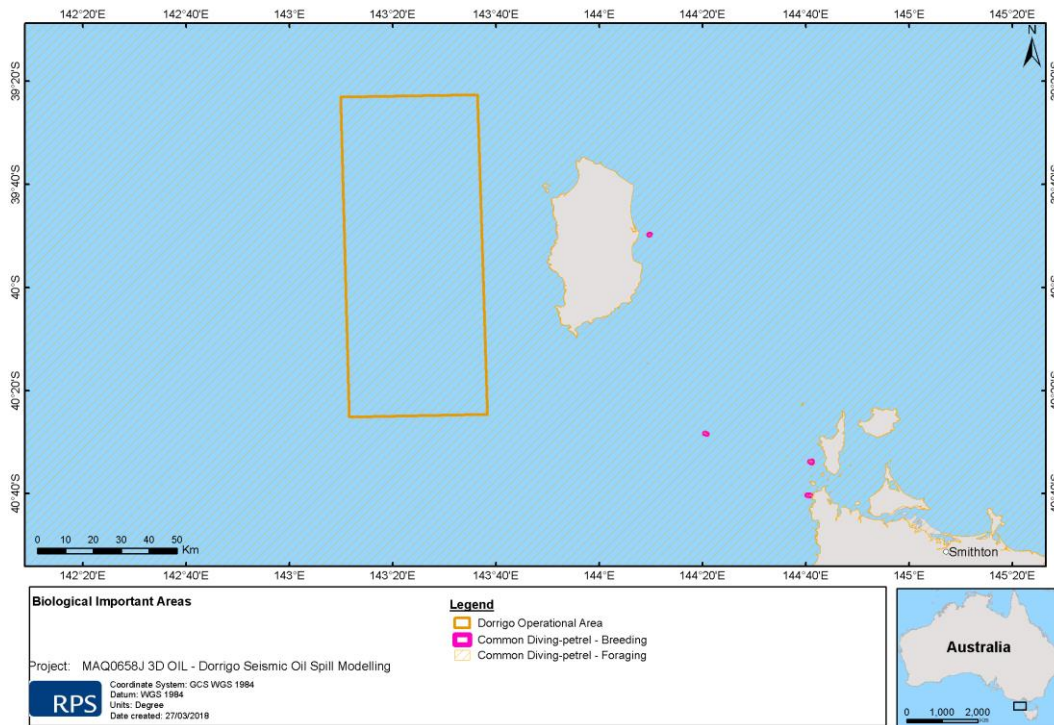
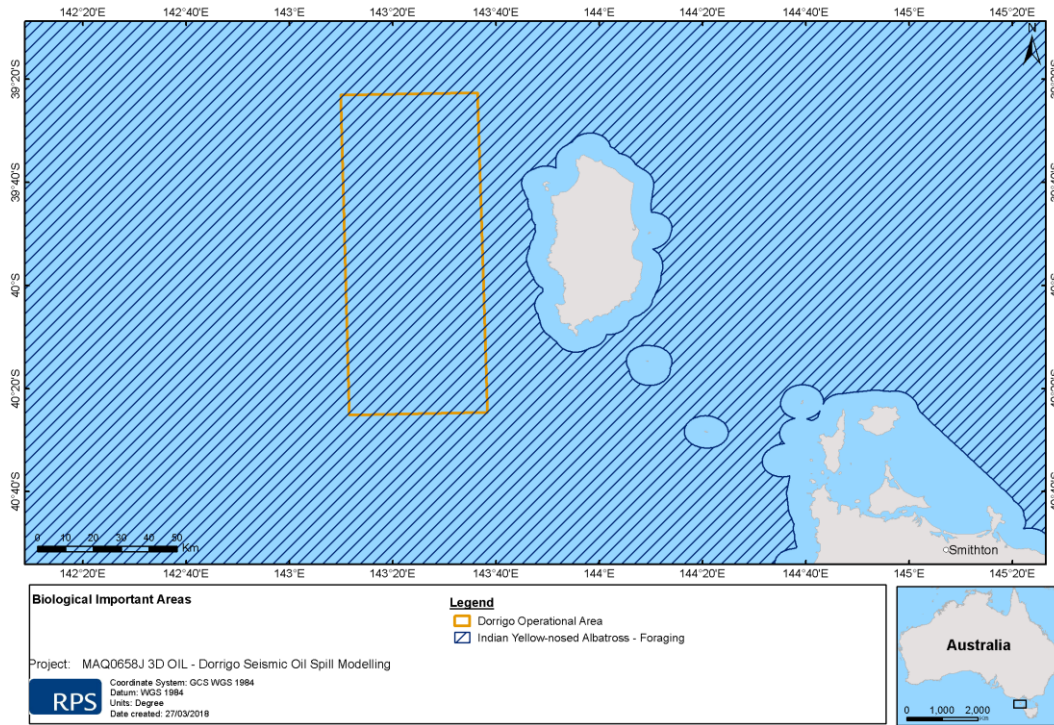
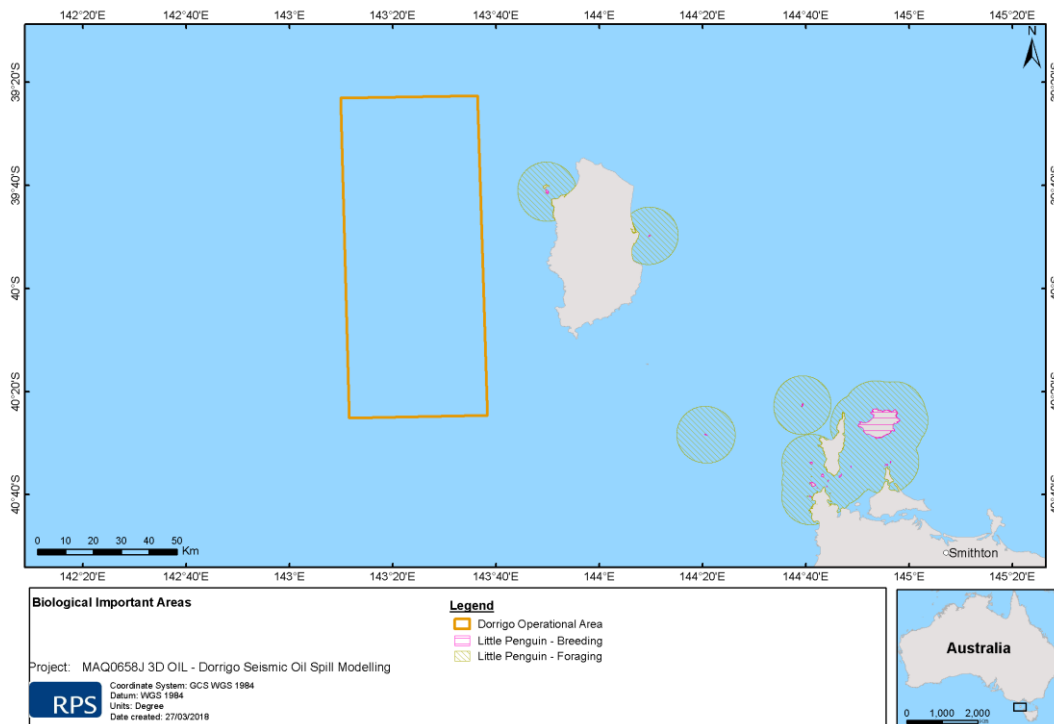


Figure 31 Biologically important areas for the common diving petrel assessed for oil exposure



**Figure 32** Biologically important areas for the indian yellow-nosed albatross assessed for oil exposure



**Figure 33** Biologically important areas for the little penguin assessed for oil exposure

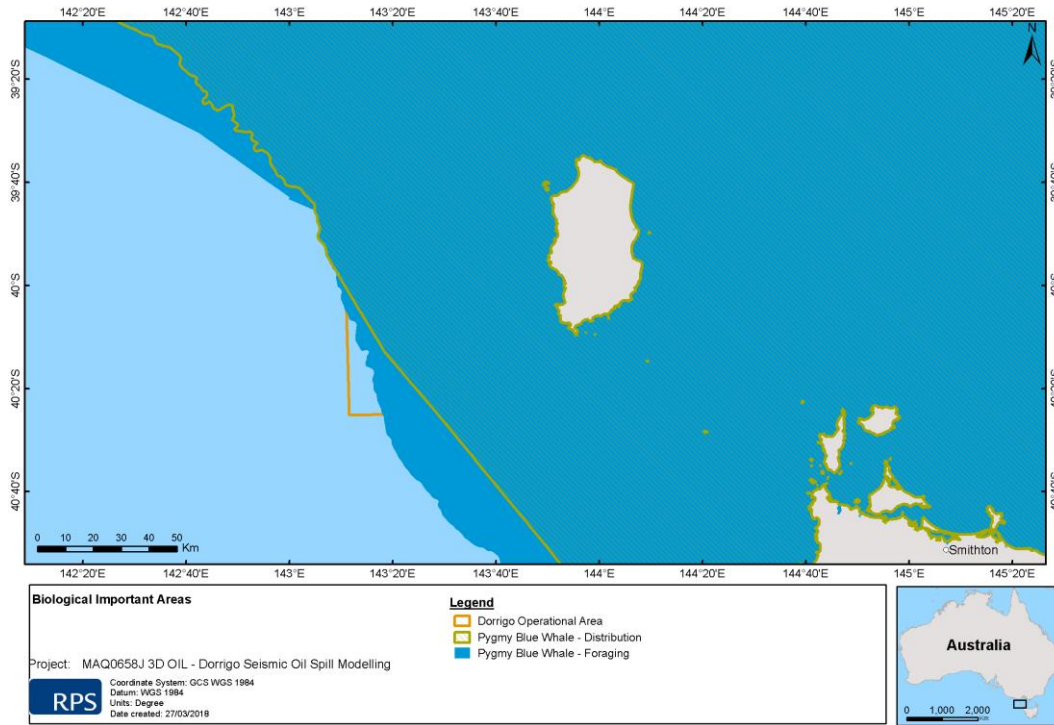


Figure 34 Biologically important areas for the pygmy blue whale assessed for oil exposure

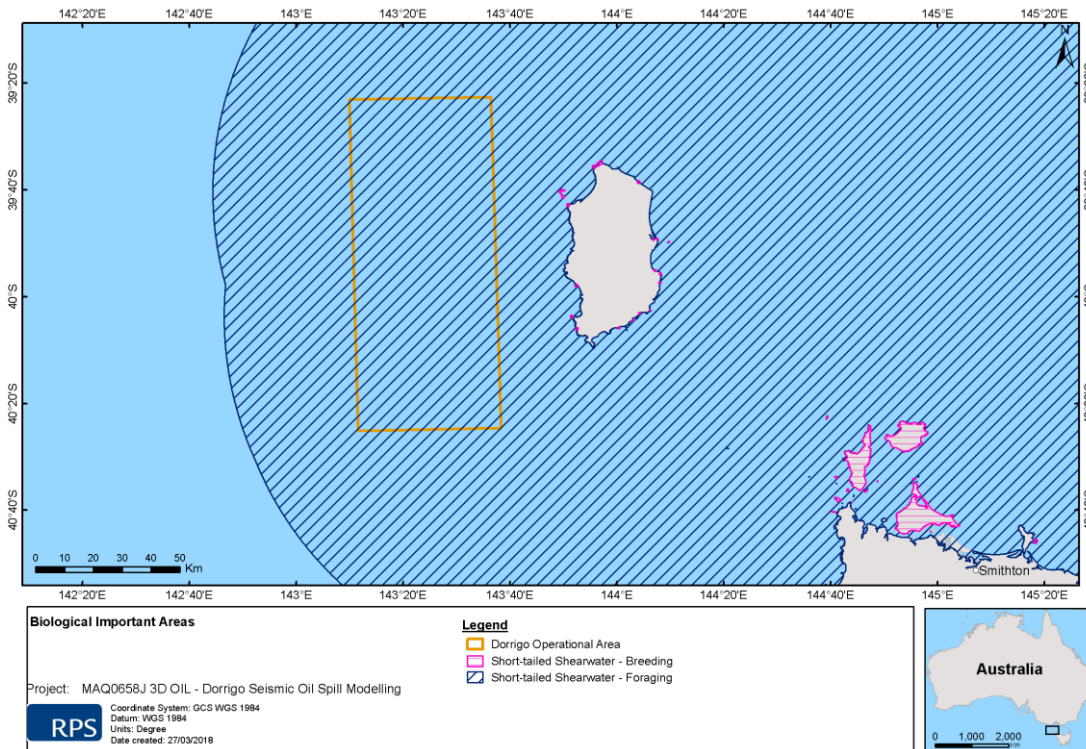


Figure 35 Biologically important areas for the short-tailed shearwater assessed for oil exposure

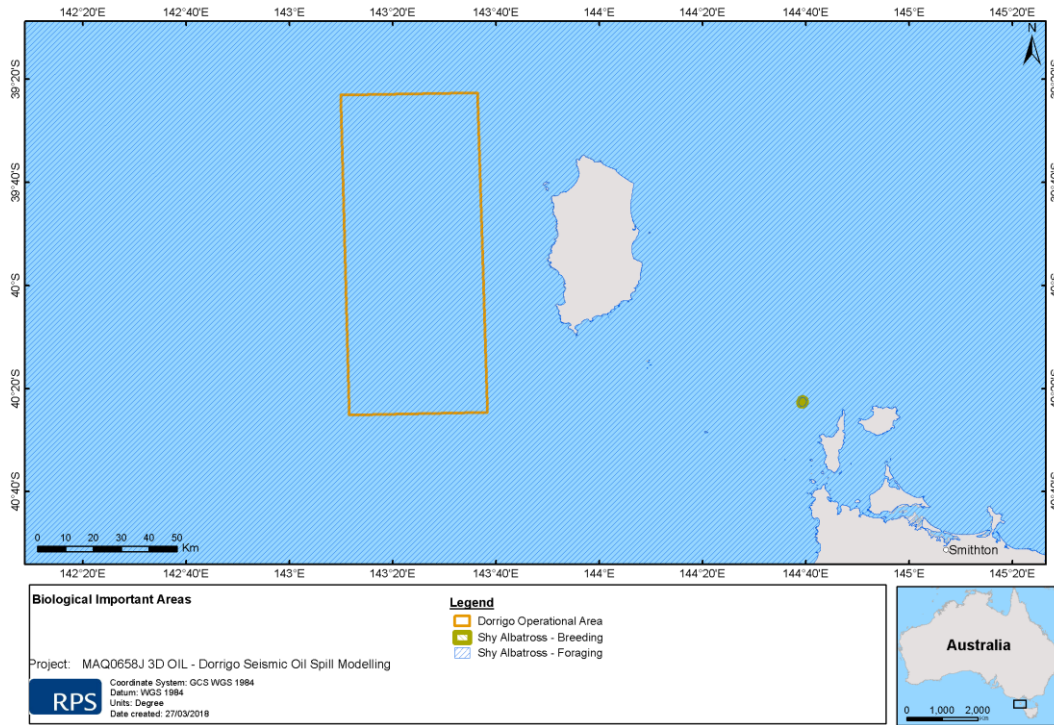


Figure 36 Biologically important areas for the shy albatross assessed for oil exposure

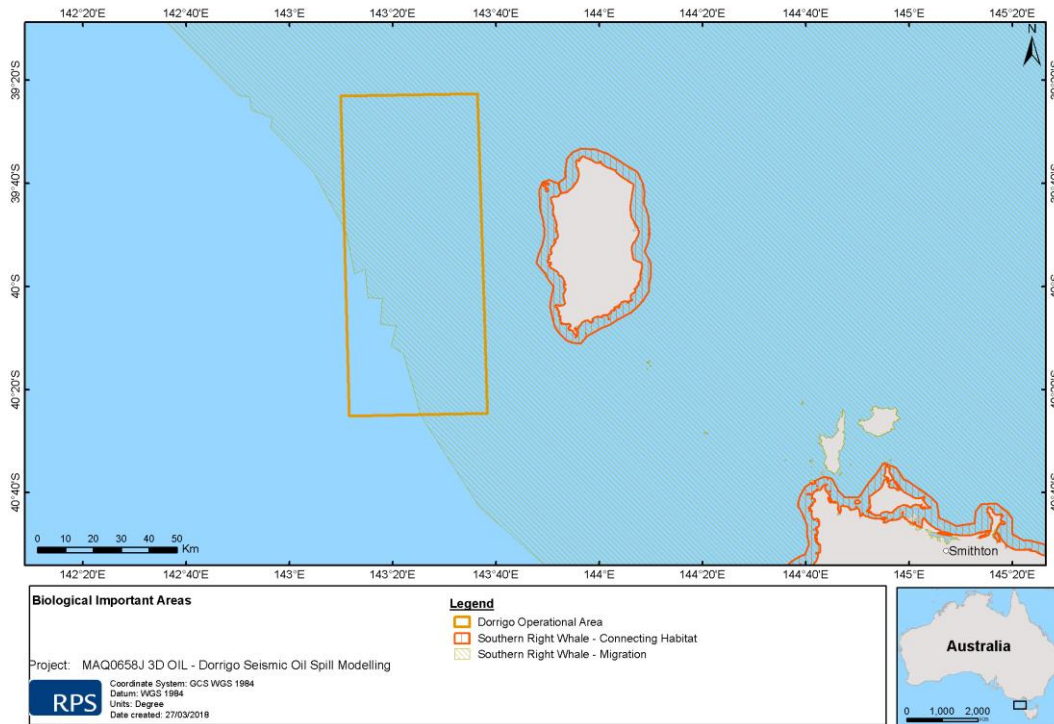


Figure 37 Biologically important areas for the southern right whale assessed for oil exposure

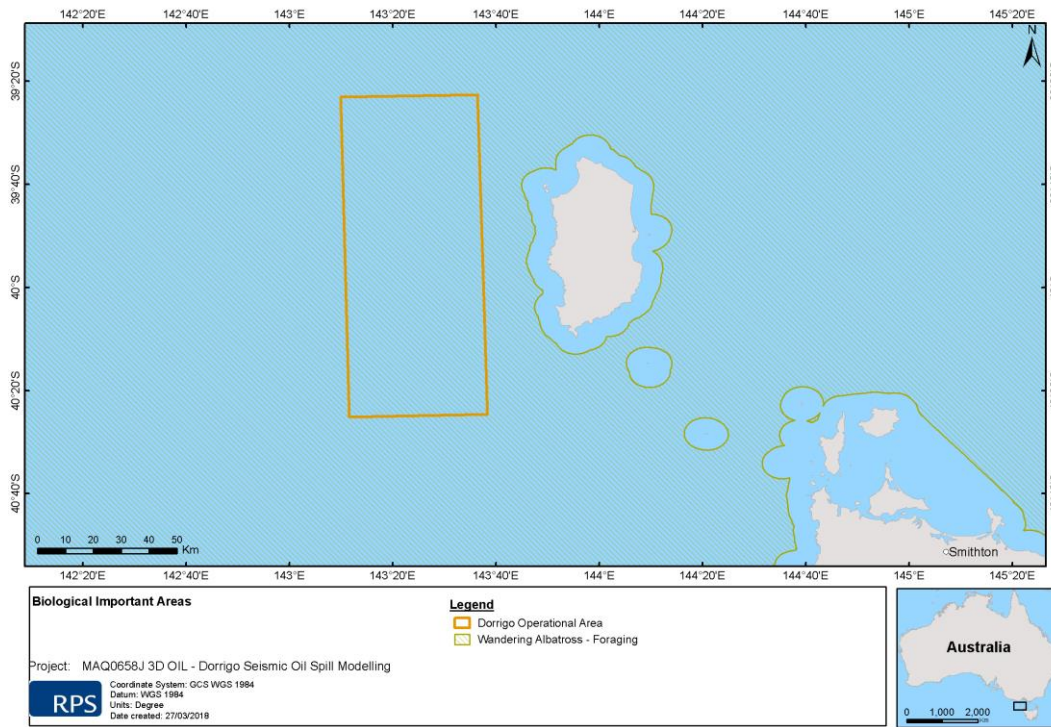


Figure 38 Biologically important areas for the wandering albatross assessed for oil exposure

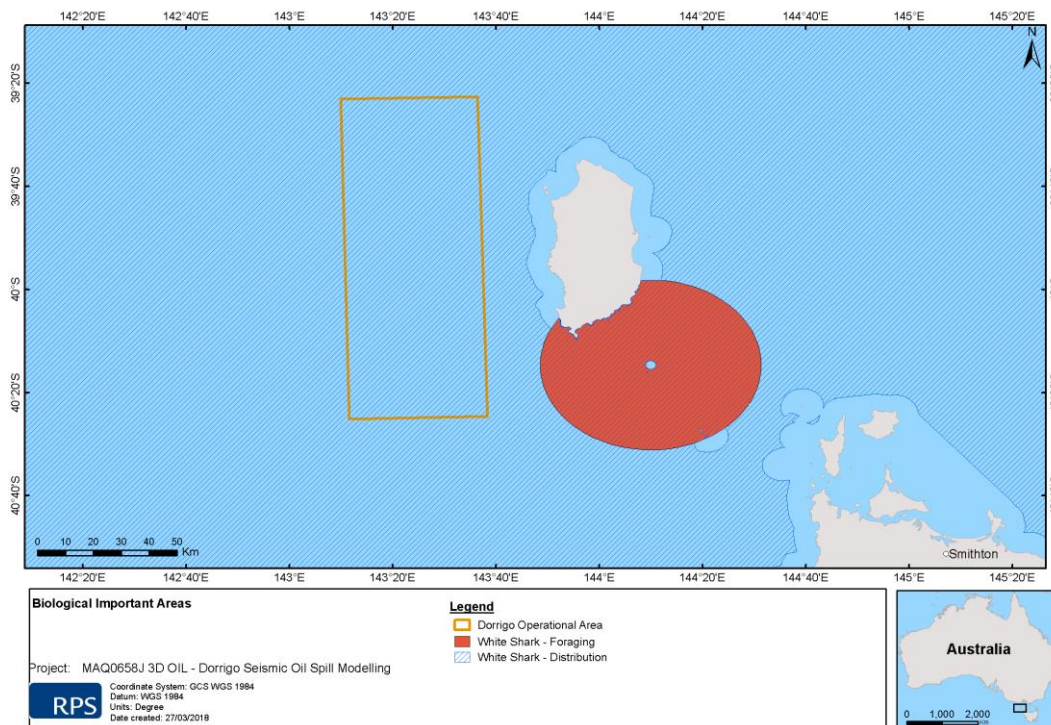
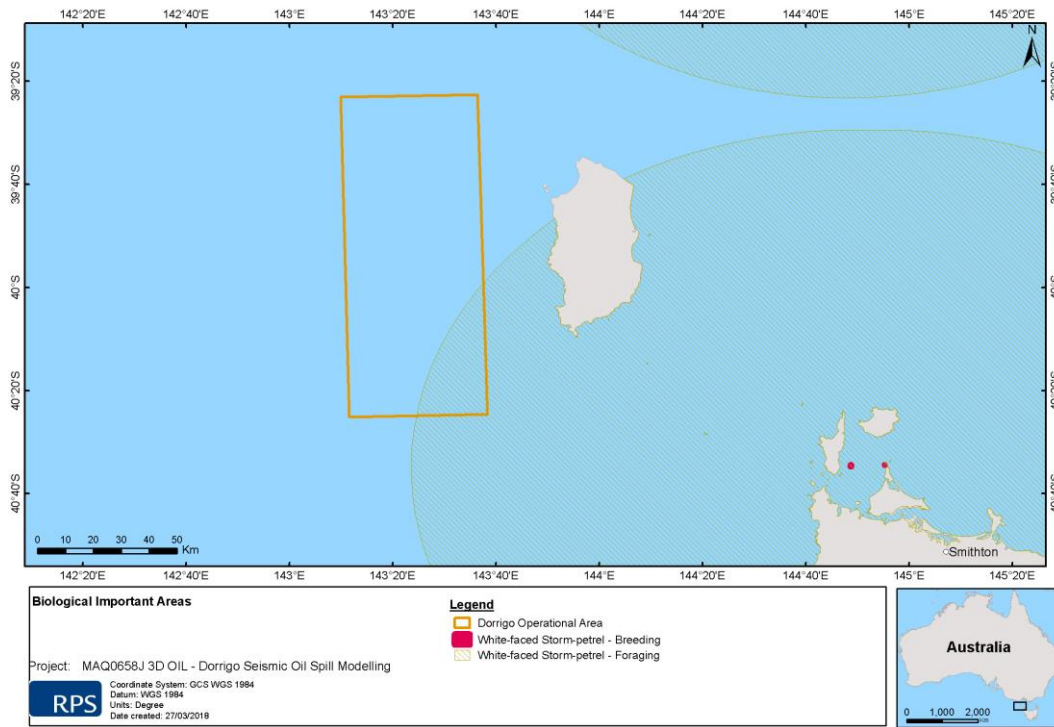


Figure 39 Biologically important areas for the white shark assessed for oil exposure



**Figure 40** Biologically important areas for the white-faced storm-petrel assessed for oil exposure